Coastal Storm Surge Identification, Classification, and Evaluation at Red Dog Dock, Alaska, 2004 - 2014

by

Adam Joseph Wicks
B.Sc., University of Victoria, 2013

A Thesis Submitted in Partial Fulfillment

of the Requirements for the Degree of

MASTER OF SCIENCE

In the Department of Geography

University of Victoria

Coastal Storm Surge Identification, Classification, and Evaluation at Red Dog Dock, Alaska, 2004 - 2014

by

Adam Joseph Wicks
B.Sc., University of Victoria, 2013

Supervisory Committee

Dr. David E. Atkinson, (Department of Geography, University of Victoria)
Supervisor

Dr. Ian J. Walker, (Department of Geography, University of Victoria)
Departmental Member

Supervisory Committee

Dr. David E. Atkinson, (Department of Geography, University of Victoria)
Supervisor

Dr. Ian J. Walker, (Department of Geography, University of Victoria)
Departmental Member

Abstract

The southern Chukchi and Bering Sea region regularly experiences powerful storms that bring high winds that cause positive and negative water level set-up (storm surges) events. Positive set-up events can cause coastal inundation, sometimes extending far inland for low-relief locations, and negative set-up events can be problematic for shallow-draft marine equipment, such as barges. A ten year record (2004-2014) of water level data is available from a NOAA tide gauging station situated at the Teck Alaska Inc. Red Dog Mine Port Facility located to the north of the Bering Strait on the southwest Chukchi Sea coast. In this thesis these data are used to develop a database of water level set-up (storm surge) events using a novel identification methodology; by adapting fundamental wind storm identification concepts used by Atkinson (2005) and applying them to a water level dataset. The surge event database is then analyzed to identify primary types of events, to derive seasonal patterns and frequencies of occurrence, and to determine likely atmospheric driving mechanisms. There were 44 surge events identified – 21 positive, 23 negative – that tended to occur during the months of November, December, and January; none were recorded in the months May through August. The event typing work suggested four distinct surge patterns. Analysis of weather drivers, performed through visual interpretation of the temporal shape/form of the events and via use of an Empirical Orthogonal Function (EOF) analysis, suggested favoured locations for storm systems – the far eastern Chukotka Peninsula for positive set up events (west of Red Dog Dock), and the Alaska Peninsula for negative set ups (south of Red Dog Dock). A

storm system situated to the west of the port generates southwest winds that drive positive set-up events, and a storm situated to the south generates easterly winds that drive negative set-up events. The sea level pressure weather patterns for positive set-up surge events are much stronger and shorter lived than for negative set-up events. This work has established an improved understanding of seasonal storm surge for the region and offers a potential basis for the improved forecasting of both positive and negative set-up surge events in the future.

Table of Contents

List of Tables

List of Figures

Acknowledgements

I would like to express my gratitude to everyone in the climate lab with a special thanks to Norman Shippee and Weixun Lu for their friendship, valued insight and discussion – I could not have done it without all of your support. A special thanks to Noah Spriggs for his assistance in the creation of a working python script.

To my friends and family – Mom, Dad, Michelle, Dylan, and Charlie and Finn – thank you for your support, patience, and understanding while working on this thesis and completing my degree.

A sincere thank you to my supervisor, David Atkinson, for his guidance, support, and direction throughout this process. Thank you to my co-supervisor, Ian Walker, for pushing me to produce the best thesis I could.

1. Introduction

The North Pacific is one of the most active storm centres in the Northern Hemisphere (Mesquita et al., 2009; Graham and Diaz, 2001). The North Pacific storm track feeds storms into the southern Bering Sea, from here a subset make their way into the North Bering - South Chukchi Sea region (Fig. 1). These storm systems can have a duration in excess of a week, varying greatly by season with summer storms tending to be shorter in duration (Mesquita et al., 2010; Bader et al., 2011). The size of a storm system can range from meso scale (< 1000km) to synoptic scale (> 1000km). Favourable upper air patterns, for example when an upper level Low is positioned to the east of a surface Low, placing a divergent region above the convergence region at the surface, sometimes result in a re-energization of storms. This can result in heavy precipitation and strong winds, which can generate severe marine states and sometimes cause coastal inundation due to storm surge.

The low-relief coastline of northwestern Alaska is particularly sensitive to high wave action. The coastal morphology of the region is one of marine deposition prograded by waves and currents. As such, this Barrier Coast does not lend itself well to the mitigation of surge forcing; instead, the low-lying littoral zone leaves the coastline exposed to high waves and flooding (Blier et al., 1997). Storm surges are linked to inland flooding and enhanced wave run-up, causing damage to coastal infrastructure, such as roads, docks, and outbuildings. (eg. Reimnitz and Maurer, 1979; Kowalik, 1984; Blier et al., 1997). These surges can have serious negative impacts on the remote coastal village communities of the region. In addition to the physical and socio-economic impacts to the villages along the coast, delicate deltaic ecological systems can also be negatively impacted by high magnitude storm surge events. The inland inundation of saltwater as far as 10km inland, can

disrupt the wildlife that rely on these northern deltaic ecosystems (Wise et al., 1981; Jorgenson and Ely, 2001).

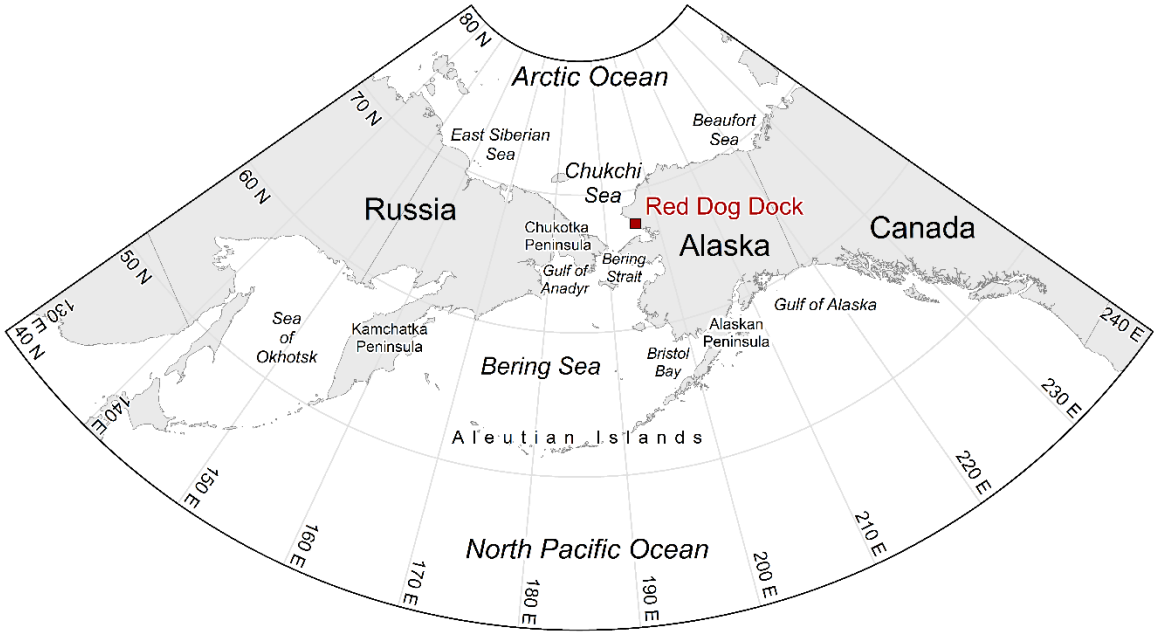

Figure 1. Bering Sea – Chukchi Sea.

1.1. Storm surge

Strong winds that can accompany extra-tropical cyclones transfer momentum and energy into the near surface layers of the ocean. On the short term this results in wave generation. If winds are able to persist, energy transfer extends into the upper layers of the ocean, which can be entrained and driven into a coastal region. The forcing is at its greatest potential when open-water fetch is maximized (Henry and Heaps, 1976; Wise et al., 1981). Wind forcing on a surface is proportional to the square of the wind speed relative to the surface (McPhee, 2008).

There are a multitude of factors at work in determining the ultimate response of surface water to high winds, such as the Coriolis force. The direction of travel of wind driven water masses is not parallel to the wind direction, but is instead angled to the right of the dominant wind direction. In the Northern Hemisphere the Coriolis force causes objects in motion to deflect to the right, as a

function of the earth's rotation (Fathauer, 1997). In the Bering Sea the net water transport is roughly 45 degrees to the right of the dominant wind vector (Fathauer, 1997).

1.2. Previous work

Early work in the region began with a study that was part of a coordinated government and industry initiative carried out in 1974-1975 known as the Beaufort Sea Project (Henry and Heaps, 1976). The study focused on producing methods to best predict sea, ice, and atmospheric conditions during the ice-free season on the Mackenzie-Bathurst shelf. They compared occurrences of surge events in ice-free and open-water conditions and concluded that wind stress is the dominant driver of surges when a shallow coastal shelf is present (Henry and Heaps, 1976).

Reimnitz and Maurer (1979) focused on a case study of a surge event in 1970 along the north coast of Alaska at Barrow, which saw a three meter meteorological tide (surge plus astronomical tide). The intent of the paper was to analyze impacts of this event and to speculate on the causes of a winter surge event when full sea-ice cover conditions were present (Reimnitz and Maurer, 1979). Through examination of the driftwood lines, coastal bathymetry of the shelf, average astronomical tidal variation, and seasonal ice coverage they surmised that a surge with a magnitude of three meters is likely to only occur once in one hundred years along the Beaufort Coast (Reimnitz and Maurer, 1979). They commented that the phenomenon of winter storm surge events under sea-ice conditions presented a gap in the literature as it was commonly accepted that sea-ice dampens wave action, limiting the severity of a surge.

In the 1980's the importance of storm surge research was directly related to the recent exploration of the North Slope oil reserves (Kowalik, 1984). Kowalik (1984) developed a numerical model to predict surge magnitude using the equations of motion for the atmosphere and ocean, which also included dynamical interactions with sea-ice. Kowalik identified an important

impact associated with negative surges in the winter; that is, their potential to cause fracturing of shorefast ice. The potential hazard of fractured shorefast ice, as a result of a prolonged high wind event (negative storm surge), can mobilize large pieces of ice and expose parts of the coastline to positive surge events. A lack of shorefast ice leaves the coast vulnerable to flood events that would have otherwise been muted by the ice.

Kowalik and Johnson (1986) extended the surge model developed by Kowalik in 1984 and applied it to the Norton Sound region of the northeastern Bering Sea. The model considered both sea-ice and surface water motion under open boundary conditions, as before, with the addition of ice-edge and fast-ice parameters. The Bering Sea model was successful in reproducing features of ice distribution and water level changes as observed during surge events at a large spatial scale; however, when applied to the smaller scale Norton Sound, the model was less successful. This was likely because, the model possessed a water depth that was too deep to allow a realistic coastal surge event to occur.

Mason et al. (1996) conducted a study using data from historic newspaper accounts of storm surge occurrence over the period 1898–1993 for Nome, Alaska. They catalogue all of the newspaper accounts of storms, and analyse the periodicity to look for patterns that align statistically with prevalent teleconnections. Their analysis showed the value in using long time series records found in historic written accounts where detailed weather records are not available. Although quantifying the surge level heights through the anecdotal accounts was not possible, they examined the frequency and periodicity of the recorded storm surge accounts.

More recently, Lynch et al. (2008) conducted a study of high wind events during the open-water season (July – November) at Barrow, Alaska. Their intent was to link high wind events in the weather forecast to the likelihood of a coastal flood event. The Polar Mesoscale Model 5

(PMM5) and the Carolina State University Coastal and Estuary Marine and Environment Prediction System (CEMEPS) storm surge model were configured for the Alaska north coast region to run simulations of mesoscale wind patterns that could result in large inundation events. The outcome of the model analysis demonstrated that forecast winds greater than 13 m s^{-1} lasting for a duration of at least 20 hours is the optimal set-up for a severe flood event, conditional on open-water surface conditions in the near-shore environment (Lynch et al., 2008).

The shallow regional bathymetry, high storm frequency, and little empirical data on storm surge activity in northwestern Alaska, provide an excellent research opportunity to study the occurrence of positive and negative surge events in the region. Analysis of data gathered at a permanent water level recording station has the potential to yield insight into regional patterns of storm surge magnitude, frequency and duration.

1.3. Study area

Alaska has one of the most rugged and complex landscapes in North America. Its coastline stretches from the temperate rainforests of its southern coast to the cold arctic plains of the North Slope. It has an active volcanic chain (the Aleutian Islands) and world renowned fishing grounds. Two-thirds of the state's population is living on or near the coast, dispersed amongst a few larger hubs and many smaller village settlements (Fathauer, 1997). Many of the northern villages in coastal Alaska still practice subsistence living and are typically very marine focused, leaving them vulnerable to coastal hazards (Jorgenson and Ely, 2001).

The study region for this thesis – North Bering and South Chukchi Seas (Fig. 1) – is centered on the Red Dog Dock located northeast of the Bering Strait on the Alaskan coastline between the towns of Kivalina and Kotzebue. The Alaskan coastline in this region is frequently subjected to storm-generated strong winds that drive storm surge and wave action. This directly impacts

villages by eroding the coastal sediment deposits compromising the low lying barrier islands on which they reside. The seasonal weather patterns in this region – in particular, storms moving up the western side of Bering Sea – commonly develop in such a way to produce a long southwesterly fetch, which results in favorable conditions for severe surge events along the northwestern Alaska coast.

1.3.1. Site location

A water level station was established at Red Dog Dock on August 21, 2003. The station is owned and maintained by National Oceanic and Atmospheric Administration's (NOAA) National Ocean Service (NOS) as part of their Water Level Observation Network. This station provides several types of data: observed water level, wind speed and direction, water and air temperature, and barometric pressure. Red Dog Dock is the port facility (Fig. 2) for Red Dog Mine, one of the world's largest open-pit zinc mines (Teck, 2013), owned and operated by Teck Alaska Inc. The Port Facility is a shallow-water lightering facility (offshore vessel to vessel loading process) that serves large bulk carriers that anchor ~5km offshore. The mine is located 144 km north of Kotzebue and 88 km from the Chukchi Sea with a 90 km gravel road connecting it to the shallow-water port (Fig. 3) that is used for staging and exporting zinc and lead ore (NANA, 2010). Red Dog Dock and the road connecting it to the mine are state-owned and only available for shipping July through October, during the 100 ice-free days that are typically available (NANA, 2010). Teck Alaska Inc. is confined to the ice-free season to ship as much product to market as possible, making severe weather and tide conditions during these times more costly to safety and productivity than for a comparable facility in the south.

Figure 2. Red Dog Port Facility lightering dock and conveyer. Both of the 5000t lightering barges are visible, docked at the end of the conveyor facility. Photo by David Atkinson 2006.

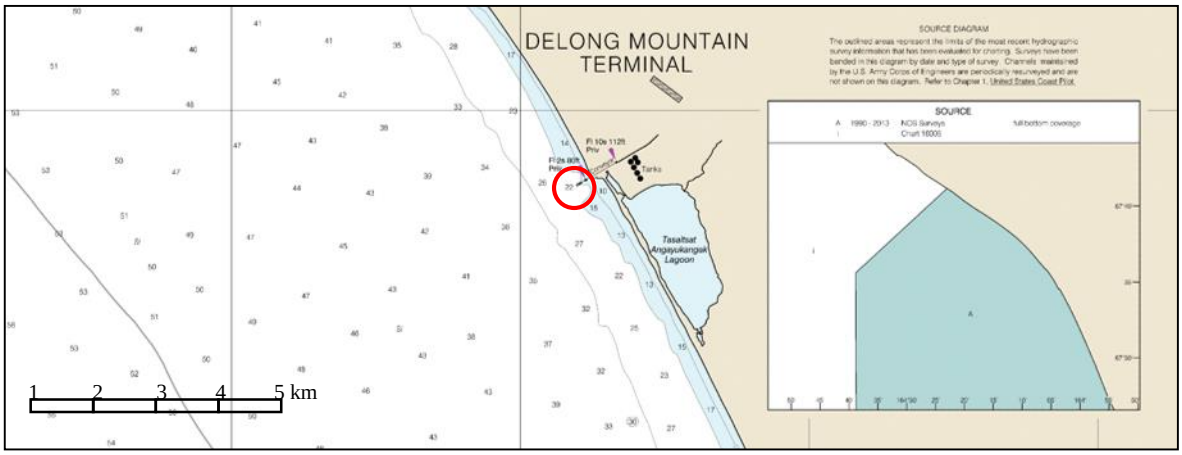

Figure 3. DeLong Mountain Terminal (Red Dog Port Facility). NOAA Office of Coast Survey Chart 16145, 2014 insert – soundings in feet. Location of Red Dog Port and conveyer pictured in figure 2 circled in red.

1.4. Thesis structure

1.4.1. Research gap

Many of the coastal village communities in northwestern Alaska rely on their location for marine-oriented subsistence living practices, and are limited in their ability to relocate. These areas are susceptible to high wave activity, strong winds and severe surge events. Little work has been done on storm surge activity, either from a modelling or observational perspective, in this region, or Alaskan waters in general. Particular storms and storm seasons have been studied, but analyses have not been done using observational data from a permanent water level recording station.

1.4.2. Purpose and objectives

This thesis is structured around two papers (Chapters 2 and 3) that focus on storm surge event identification and classification, as well as the identification of weather patterns that drive surges. Chapters 2 and 3 are written to be stand-alone manuscripts, so there is some repetition of introductory and background material. The introduction (Chapter 1) situates the research within the broader context of storm surge research in western Alaska and Sub-arctic regions. The concluding remarks (Chapter 4) provide an overview of the papers and synthesizes key results. Note that figures are consecutively numbered over the entire document.

The purpose of this research is to develop a storm surge climatology from observational water level data in order to describe seasonal patterns, overall frequency, and atmospheric driving mechanisms for storm surge events at the Teck Alaska Inc. Red Dog Port Facility on the southwestern Chukchi Sea coast, Alaska. Chapter 2 describes the development and application of a surge identification algorithm that uses a time-series trace of water level data. Results were classified by form, including nature of onset, peak, and decline. Specifically, the objectives of this chapter are to: (i) Develop a water level set-up identification algorithm, (ii) Identify surge events

from time-series data and compile a database of individual events, (iii) Classify the identified surge events into similar categories based on form, (iv) Identify atmospheric driving mechanisms responsible for the various types of surge events, and (v) Summarize emergent patterns in the surge data.

Chapter 3 examines atmospheric forcing of surge events by identifying primary atmospheric patterns associated with the major surge-type categories. Specifically, the objectives are to: (i) Examine atmospheric forcing patterns that are linked to storm surge events and analyze the relationships, and (ii) Summarize dominant atmospheric surge patterns and synthesize key findings to establish commonalities between events.

2. Identification and classification of storm surge events at Red Dog Dock, Alaska

2.1. Abstract

Powerful storms in the Bering and Chukchi Seas west of Alaska regularly bring high winds that drive positive and negative water level set-up events (storm surges). Positive set-up events can cause inundation of coastal regions, sometimes extending far inland for low-relief locations. A ten year record (2004-2014) of water level data from Red Dog Dock located to the north of the Bering Strait on the Alaskan coast was analyzed for observed severe set-up events. A climatology of events was developed, in which event occurrences were grouped by temporal evolution of the event. This suggested four distinct event types. The primary synoptic control on these events is the orientation of the pressure gradient caused by the passage of low pressure systems. The orientation of the pressure gradient, and therefore dominant wind direction, determine the magnitude, duration, and set-up (i.e. positive or negative) of a surge event. The climatology resulted in 44 observed events – 21 positive, 23 negative – that tended to occur during the months of November, December, and January. It was also noted that surges regularly occurred under less favorable conditions, when sea-ice cover is present.

2.2. Introduction

The North Bering - South Chukchi Sea region (Fig. 1) experiences frequent storms (Mesquita et al., 2009; Graham and Diaz, 2001) that bring strong winds, which can often persist when the storms stall over the region. Strong winds generate high wave states and can entrain and drive large volumes of water towards or away from shore – positive or negative set-up – depending on wind direction. Waves and storm surge are responsible for erosion and inundation problems which are a major concern for many northwestern Alaska communities where low relief and poorly consolidated sediments enhance susceptibility (e.g. Henry and Heaps, 1976; Wise et al., 1981; Mason et al., 2012). The northwestern Alaskan coastal regime is highly dynamic and experiences episodic periods of accelerated erosion from high wave action associated intense storm systems. This results in damage to infrastructure and land, such as roads, docks, outbuildings, and permafrost. (eg. Reimnitz and Maurer, 1979; Kowalik, 1984; Blier et al., 1997). The western Alaska coast north of the Yukon-Kuskokwim Delta is a micro-tidal environment. The southern Chukchi Sea region experiences a tidal range of approximately 30cm, which makes a surge level greater than 3 times the normal water levels a concern for the communities located along the coast.

Previous studies have looked at high wind events (eg. Bond et al., 1994; Pirazzoli, 2000; Atkinson, 2005; Verdy et al., 2013), specifically during the open water season (July – November) (Lynch et al., 2008). The idea is to link high wind events to the particular storm systems, or "storminess" in general, using the assumption that storm systems produce strong winds. MacClenahan et al. (2001) applied a computer based algorithm to wind speed and duration using weather station data in order to identify storm signatures and categorize several types of coastal storms. While this sort of approach can provide a good surrogate for estimating positive and negative surge event occurrence over large areas, direct water level observations represent the best

source of detailed temporal information to relate surge events to their associated atmospheric drivers.

Water level data recording stations are not common in northern regions because sea-ice makes installation of coastal equipment problematic, and the heavy infrastructure needed to facilitate such installations, such as at port facilities, is rarely present. The DeLong Mountain Terminal, the Port Facility that serves Tech Alaska Inc.'s Red Dog Mine in northwestern Alaska, has housed a National Oceanic and Atmospheric Administration (NOAA) water level recorder since 2004. These data are easily accessible and have not been previously studied for surge events. Given this, there are two objectives for this work. First, develop an identification algorithm by which surge events can be identified from a continuous time series of water level data. Second, to use the results from the identification algorithm to establish a baseline of surge activity by developing a climatology of event type and frequency, subdividing counts by open-water and ice-covered time frames.

2.2.1. Surge event drivers

Surge events result from atmospheric forcing via the action of wind, which translates into a direct relationship with atmospheric pressure patterns during surge events (Trigo and Davies, 2002). Large low pressure systems (storms) generate high winds, which in turn "force" the sea surface via the transfer of momentum driving high wave states. Given enough persistence, winds can entrain the top layers of water and drive large volumes of water into the coast (positive wind set-up) or away from the coast (negative wind set-up). These effects can cause a physical response along the coast in the form of sea level rise (or drop). This response is referred to as a storm surge and is typically observed as severe high/low residual water levels, defined as the difference between the observed water level and the predicted astronomical tide (Blier et al., 1997).

The magnitude and intensity of atmospheric pressure patterns acting on the surface sea state is known as the primary factor controlling the occurrence of surge events; variations in wind speed, duration, fetch direction, and the coastal environment (coastline orientation) are also important factors considered. The coastal environment, such as the coastal morphology and bathymetry in the region have a direct effect on the intensity and magnitude of surge events. These are important considerations for the Bering/Chukchi Sea region because the northern Bering Sea and all of the Chukchi Sea are littoral shelves where the coastal regions present as being very shallow over long distances from the coast; this can intensify a positive surge magnitude.

2.3. Methods

2.3.1. Station description

NOAA has operated a tide gauge and meteorological observation station at Red Dog Dock on the northwestern coast of Alaska (Fig. 1) since 2004, making it the most northerly water level station operated by NOAA (other than a water level facility that was operated at Barrow from 2008-2010 (Sprenke et al., 2011)). Red Dog Dock is located on the southeastern coast of the Chukchi Sea, mid-way along a 190 kilometer stretch of southwest facing coastline. A shallow ocean shelf gradually decreases offshore to a depth of 40m at the Bering Strait, reaching 50m at the deepest point. The low-lying coastal relief consists of sandy embayments, barrier islands, inlets, and wide delta mouths, all exposed to strong wave action (Atkinson et al., 2011; Mason et al., 2012). The nearest community Kivilina, a hamlet of approximately 350 people located 13km along the coast to the northwest of Red Dog Dock, resides on a small exposed strip of land that experiences frequent storms and sure events (Fig. 4).

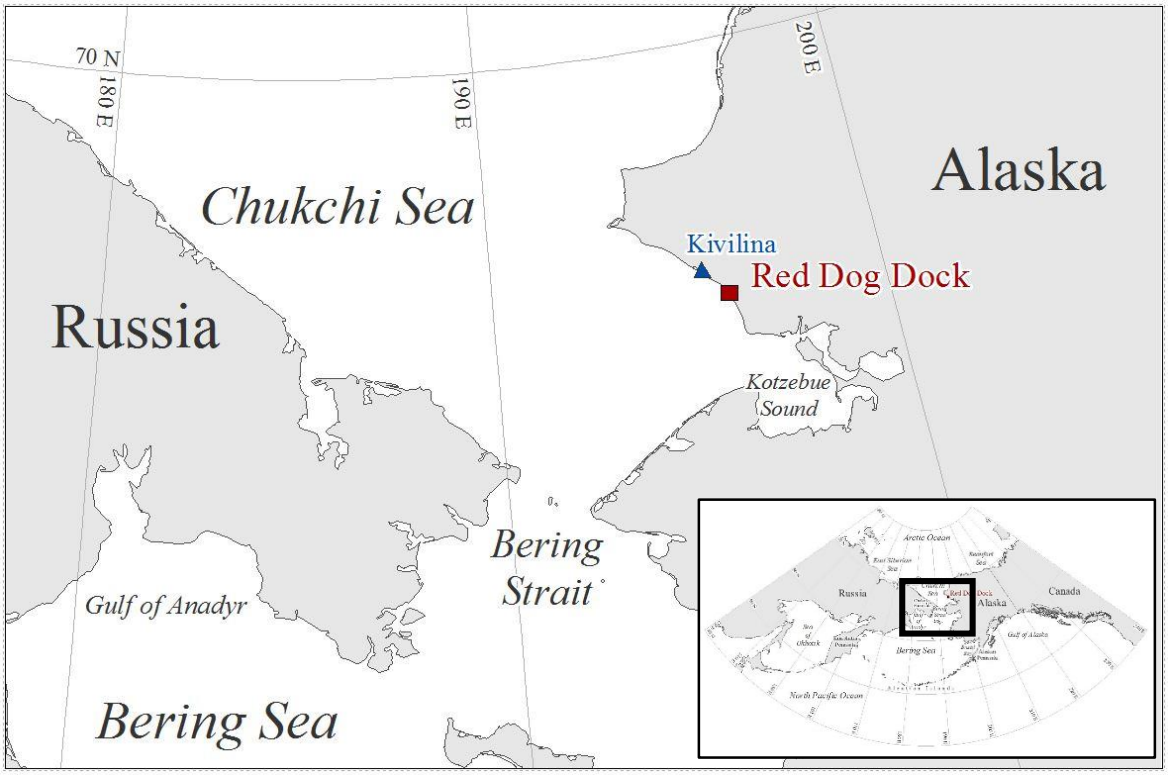

Figure 4. Geographic location of NOAA's Red Dog Dock, Alaska tide gauge, meteorological observation station, and nearest community to the observation station – Kivilina, Alaska. Insert shows regional extent.

2.3.2. Water level and meteorological data

Observed water level data were acquired from NOAA/NOS/CO-OPS (National Oceanic and Atmospheric Administration/National Ocean Services/Center for Operational Oceanographic Products and Services). These data are available since July 2004 at Red Dog Dock, Alaska station 9491094.

The meteorological data used to categorize atmospheric forcing in the region were Sea Level Pressure (SLP) gridded data from the NCEP/NCAR (National Center for Environmental Prediction/National Center for Atmospheric Research) Reanalysis 1 project (Kalnay et al., 1996). These data were accessed through the website hosting the datasets, maintained by NOAA/OAR/ESRL (Ocean and Atmospheric Research/Earth System Research Laboratory) PSD

(Physical Sciences Division (http://www.esrl.noaa.gov/psd/). These data are available at six hour intervals since January 1948 at 2.5˚ latitude/longitude resolution globally; the data were clipped to the Bering Sea region at 40˚N to 80˚N and 130˚E to 240˚E.

In addition to the water level and SLP data, sea-ice concentration data were obtained from the High Resolution Blended Dataset (Reynolds et al., 2007), also accessed through the NOAA/ESRL website. These data are available at a temporal resolution of one day and a global spatial resolution of 0.25˚; for the purpose of this study the gridded data are constrained to the Bering Sea region at 50˚N to 80˚N and 150˚E to 240˚E.

2.3.3. Data preparation

The NOAA water level recording gauge is situated on one of the pylons supporting the Red Dog Port conveyor system (Fig. 2). Observations are recorded every 6 minutes; for this project hourly water level data are used. The data record extends from August 21, 2003, to the present, with two major gaps (> 1 week) occurring early in the dataset October to July 2003/2004 and August to October 2004 – and a minor gap (< 1 week) in December 2005. These gaps in the start-up years of the station do not adversely impact the study for a couple of reasons: the August to October period tends to be one of lower storm frequency, than the winter, for example; the gap in December is short; and, the study period begins July 2004.

Water level data at this site are referenced to the datum established by NOAA for this location, termed the Red Dog Dock station 9491094 datum ("STND" zeroed at 0.00 meters), which in turn is calibrated to the North American Vertical Datum of 1988 (NAVD88) calculated over NOAA's present epoch (1983-2001). NOAA's present epoch is applied to all of their tide gauge stations, it includes all significant tidal fluctuations based on a 19 year period in order to best match the 18.6 year lunar nodal cycle (Evans et al., 2003). For this study residual water level values are used.

These values are defined as the verified observed water levels less the expected astronomical tide, such that the residual values reflect only the non-astronomical component of the water level fluctuations.

The water level data are analyzed using a modified version of Atkinson's (2005 – A05) – strong wind event identification algorithm. He used a multi-stage algorithm to identify storm events from temporally sequential wind observations. Wind events exceeding a user defined threshold were identified and isolated for discrete storm events. Using a similar algorithm surge events are identified here. To target strong negative and positive set-up surge events Atkinson's method was altered to fit the nature of water level observations. The surge event identification algorithm is detailed below, but in general operates by identifying peak water level occurrences that exceed a user-specified threshold on an hour-to-hour basis. Identified occurrences are extracted and placed in a database that includes start date-time, end date-time, peak magnitude, and characteristics that include: onset duration, peak duration, return duration, and total duration.

2.3.4. Surge event identification

Establishing a database of surge events is grounded in the assumption that it is important to define the duration of a given event. The classic Pareto peaks-over-threshold approach (eg. Simiu and Heckert, 1996) is not used because the intent was to develop an algorithm that provides results that can be more readily associated with synoptic drivers.

The surge event identification algorithm is structured around three passes through the dataset, as follows. A first pass considers each datum in isolation; any datum exceeding a "trigger" threshold is tagged. A second pass is then made through both the water level data and the tagged dataset creating a dataset containing all the residual values above the threshold value. A final pass is made applying a series of contextual decisions to identify the full duration of the discrete set-up

event start and end times. The events are indexed and recorded in a database. Detailed algorithm operation is outlined below.

The initial pass applies a simple true/false binary assignment to identify values as being above or below the threshold. The second pass populates an empty dataset with the original water level data values where the initial pass is true, and zeros where false. Once the events are identified a series of contextual rules are applied, starting with an examination of the discrete groupings of water level data values over the threshold. If the duration between data values from two discrete groupings is less than a specified "lull" interval, the two groupings are considered to be the same event. If the duration between the two discrete groupings exceeds the lull interval, the data value is then examined. If the value does not drop below a secondary "continuity" threshold, the groupings are also considered to be the same event. If the data value does drop below both thresholds and exceeds the lull interval the grouping is considered to be two separate events.

It can also be the case that an event does not start or stop rapidly, instead exhibiting distinct "shoulder" periods where the water level is elevated above astronomical tide levels, yet not above the algorithm threshold. In addition to the shoulder period, a "chute" rule is applied where the onset and return duration are evaluated to include the water level data values a number of consecutive observations once the data values drop below the thresholds. Thus, the following parameters must be specified in the algorithm to identify positive and negative water level set-up events: trigger threshold (T), lull duration (L), continuity threshold (C), shoulder period (S), and chute rule (R) (Fig. 5).

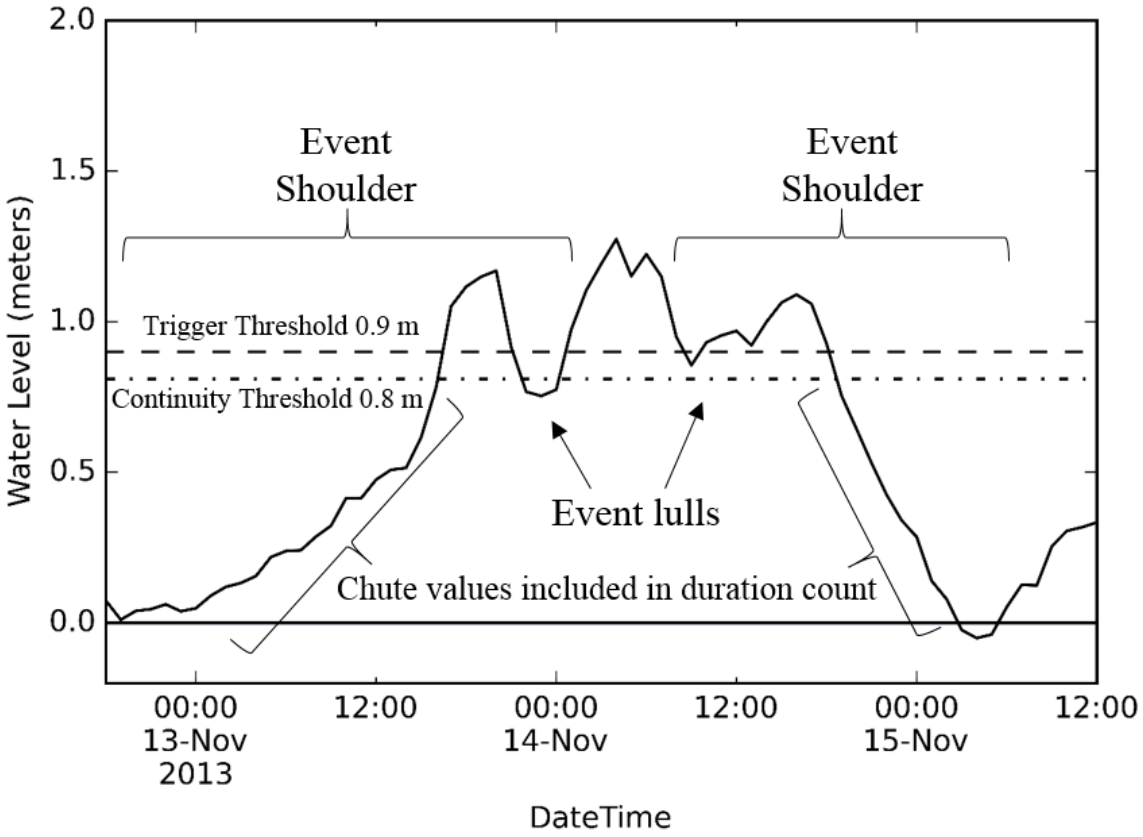

Figure 5. Surge event algorithm definition depicting parameters used for identifying a single surge event.

The selection of appropriate values for the parameters identified above depended upon a certain amount of visual fine tuning; that is, in most cases the occurrence and duration of a set-up event was fairly apparent by examining the residual water level trace. In order to establish an initial baseline the parameters were assigned "first-guess" values T = 1 m, C = 0.8 m, L = 6 h, R = 48 steps, and S = 100 h, arrived at after exploring the dataset as a whole. Application of the algorithm using these parameter settings captured a number of events, however the duration of many of the events was far too great and these settings failed to distinguish concurrent events as unique set-ups. Sub-setting the data by year allowed for the parameters to be more easily refined. Repeated trial and error alterations resulted in the following parametrization: T = 0.9 m, C = (0.9*T) m, L = 6 h, R = 9 steps, S = 12 h. These parameters provided the optimal representation of a positive and

negative set-up event. The continuity threshold was changed to a percentage of the trigger threshold in order to increase the fine tuning ability of the algorithm. Having the continuity threshold as a function of the primary threshold allowed for increased ease in the refinement of an appropriate trigger threshold. The lull duration remained the same, as variations in this parameter had little impact on the effectiveness of the algorithm, since it is largely dependent on the difference between the continuity and primary threshold values. The chute and shoulder parameters had the greatest impact on the output, since they are responsible for defining the surge response durations. Ultimately, a chute value of 9 intervals and shoulder duration cut-off limit, once the continuity threshold is crossed, of 12 hours provided the best coverage of an event onset and return; this was the greatest interval possible that would not result in a potential overlap of multiple events that occur in short succession.

Positive and negative set-up events were also classified according to sea-ice concentration (open-water verse ice-covered). NOAA "mean ice percent" charts depicting daily sea-ice concentration were obtained and used to determine the sea-ice conditions at the time of the event. Two values were retained, one for sea-ice conditions to the northwest of the Port Facility, and the other for sea-ice conditions to the southwest (see Table 1).

From the resulting database the following summary parameters are extracted: total count of events, positive verse negative set-up count, open-water verse ice-covered count, peak magnitude, mean peak magnitude, and mean duration. In addition to total count, overall mean duration, and presence or absence of regional sea-ice, the surge events are compared year-to-year, season-to-season, and month-to-month.

2.3.5. Classification of surge events

Once each of the individual surge events are identified it is possible to group them into major types according to the shape described by the pattern of the temporal evolution of the water level response. The typing process works by taking an initial consideration of each event to define how rapidly water level changes in the beginning phase of the event, the nature of its duration, and how rapidly water level changes as the event ends. To visualize the shape and define the duration straight lines are drawn backward from the peak to the beginning of the onset and forward to the end of the return. In some cases, a distinct plateau was noted, in which case a roughly horizontal line was added. The events that have similar temporal patterns are grouped together and analysed to give an overall description of each type. The form and a detailed description of each type is presented in the results section. The durations for the categories onset, peak, and return are calculated by averaging both the positive and negative set-ups together as both follow a similar temporal pattern.

2.4. Results

44 surge events were identified, 21 positive set-up and 23 negative set-up (Table 1). At least one event was observed in each month over the September through April time frame, a period that includes both open-water and ice-covered conditions. The greatest magnitude positive event (2.23m) occurred on February 25, 2011 under full regional sea-ice coverage. In contrast, the greatest magnitude negative event (-1.84m) occurred November 9, 2005 under open-water conditions.

Table 1. Storm surge event dataset 2004 - 2014. Data are organized by year (July 1 to June 30) and month. Fetch direction relative to Red Dog Dock and sea-ice coverage expressed as daily mean sea-ice concentration (concentration >50% are shaded blue), type classification refer to section 2.4.4.

Year	Month	Duration (h)	Peak Magnitude (m)	Positive / Negative	Dominant Fetch Direction *Fetch SW 600km/NW 800km*		Type
					Open-Water	Sea-Ice	
2004	October	65	1.43	Positive	SW/NW		B
2004	November	43	-1.14	Negative	SW/NW		A
2004	November	34	-0.92	Negative	SW/NW		A
2004	November	33	0.98	Positive	SW	NW	A
2004	November	34	0.95	Positive	SW	NW	A
2004	December	53	-0.96	Negative	SW	NW	C
2004	December	44	1.84	Positive		SW/NW	B
2005	January	65	1.47	Positive		SW/NW	B
2005	January	36	0.97	Positive		SW/NW	C
2005	September	40	1.34	Positive	SW/NW		A
2005	***November***	***115***	***-1.84***	***Negative***	***SW/NW***		**B**
2005	November	121	-1.67	Negative	SW/NW		D
2006	February	77	1.16	Positive		SW/NW	C
2006	November	72	-1.13	Negative	SW/NW		D
2006	November	64	1.21	Positive	SW/NW		B
2007	January	41	-1.03	Negative		SW/NW	B
2007	March	80	-1.44	Negative		SW/NW	C
2008	January	56	1.47	Positive		SW/NW	A
2008	October	46	-1.37	Negative	SW/NW		A
2008	October	42	0.95	Positive	SW/NW		A
2008	November	37	-0.96	Negative	SW/NW		A
2008	December	56	-1.19	Negative		SW/NW	A
2008	December	36	1.06	Positive		SW/NW	A
2009	March	45	1.11	Positive		SW/NW	A
2009	March	68	-1.04	Negative		SW/NW	B
2010	January	49	-1.14	Negative		SW/NW	A
2010	April	36	0.91	Positive		SW/NW	C
2010	December	48	-1.14	Negative	SW	NW	C
2010	December	101	-1.45	Negative	SW-partial	NW	B
2011	February	44	1.45	Positive		SW/NW	B
2011	***February***	***88***	***2.23***	***Positive***		***SW/NW***	**D**
2011	March	51	0.99	Positive		SW/NW	A
2011	September	75	-1.32	Negative	SW/NW		B
2011	November	38	1.46	Positive	SW/NW		A
2011	December	29	-1.02	Negative		SW/NW	A
2011	December	38	-0.98	Negative		SW/NW	A
2012	October	64	1.01	Positive	SW/NW		C
2012	November	67	-1.13	Negative	SW/NW		C
2012	December	45	-1.07	Negative		SW/NW	C
2013	January	40	-1.10	Negative		SW/NW	A
2013	November	76	1.55	Positive	SW/NW		C
2013	November	45	1.27	Positive	SW/NW		C
2013	December	46	-0.97	Negative	SW	NW-partial	C
2014	January	59	-1.49	Negative		SW/NW	A

2.4.1. Event counts

The mean annual event count is 4.4 with a maximum of 9 in 2004 and a minimum of 1 in 2007 (Table 2). Mean annual counts are well distributed between positive (2.1) and negative (2.3) set-up events. The mean event count by month (Fig. 6) shows the greatest likelihood of an event occurring in the months of November and December, with events occurring as early as September and as late as April. No events were observed in the May through August timeframe over the ten year period of record. A plot of positive and negative event counts by month (Fig. 7) shows that either type occurs with equal frequency during the SON period, a greater potential of a negative event occurring in NDJ, and an increased likelihood of a positive event occurring in JFMA.

Table 2. Mean number of surge events including annual positive and negative counts. Stacked bar plot of positive and negative surge events observed at Red Dog Dock, Alaska, 2004-2014.

Year	Count	Positive	Negative
2004	9	6	3
2005	4	2	2
2006	4	1	3
2007	1	1	0
2008	7	3	4
2009	2	1	1
2010	5	3	2
2011	4	1	3
2012	4	1	3
2013	4	2	2
mean	**4.4**	**2.1**	**2.3**

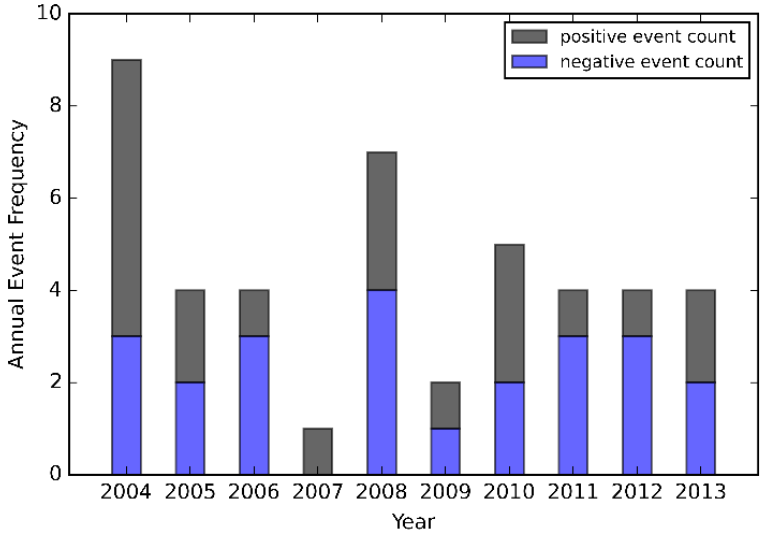

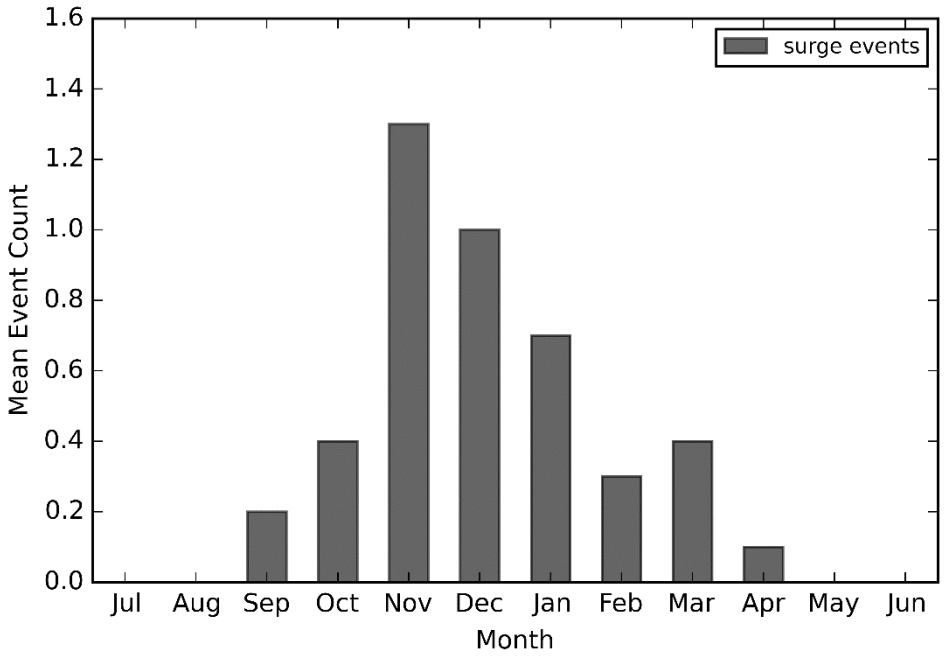

Figure 6. Mean event counts by month.

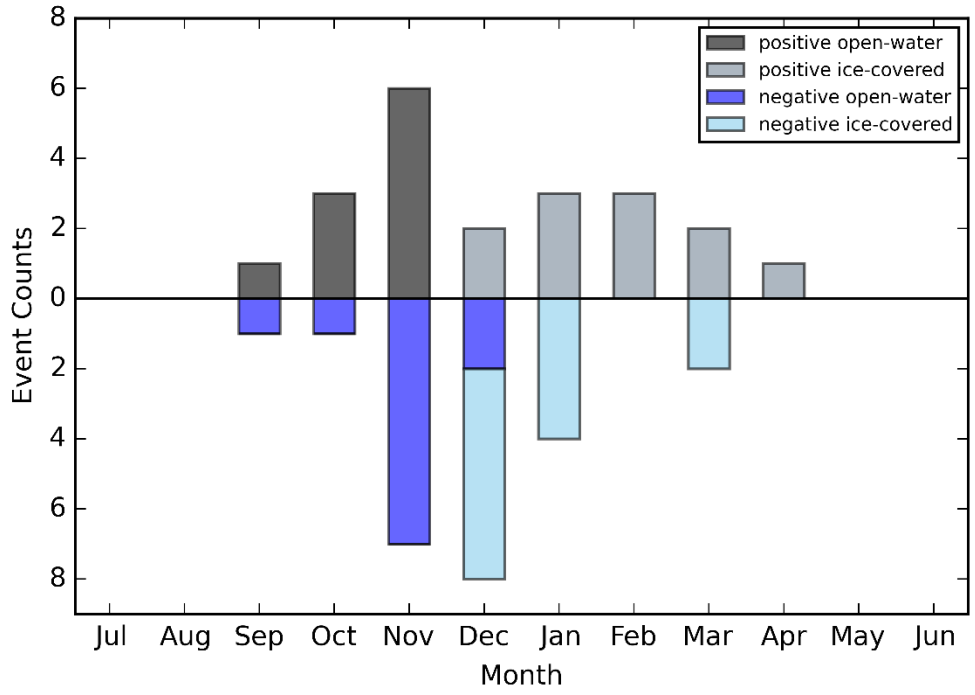

Figure 7. Event counts positive and negative including open-water verse ice-covered.

2.4.2. Peak water levels

Negative and positive set-up event counts (21, 23) and mean values (1.3m, -1.2m) show a relatively even distribution in terms of when events occur and their magnitudes (Table 3). The largest positive set-up (2.23m) occurred in February during full sea-ice coverage. The peak negative set-up (-1.84m) occurred in November under mostly open-water conditions.

Table 3. Descriptive statistics of positive and negative surge events; count is the total number of events over the ten year study period, mean is calculated using the peak magnitude (metres) of each positive and negative event.

	Positive Events	Negative Events
Count	21	23
Mean (m)	1.3	-1.2
Peak Magnitude (m)	2.23	-1.84

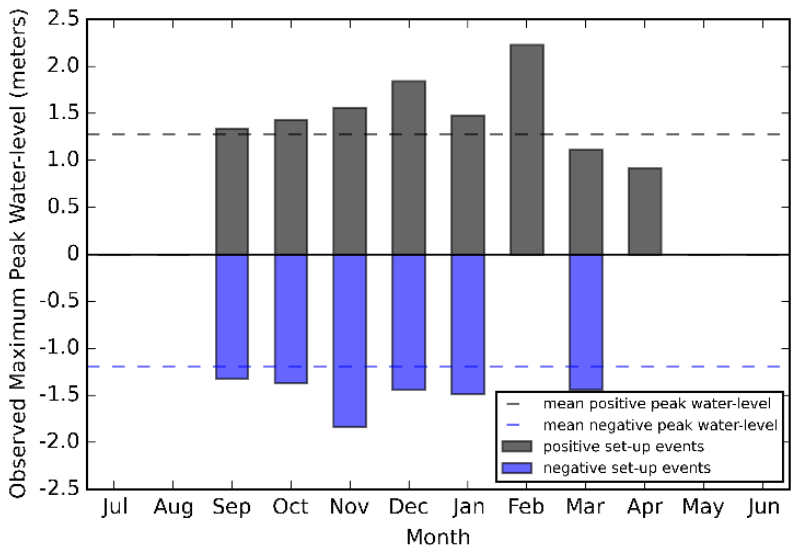

2.4.3. Surge event duration

The overall mean duration for an event (either positive or negative set-up) is 55.5 hours, with February exhibiting the longest mean duration (of either a negative or positive set-up) at 70 hours and April the shortest at 36 hours (Table 4). The negative set-up events have a much larger standard deviation than the positive set-up events: 25 and 16 hours, respectively. This difference indicates there is a greater variability in the duration of negative set-up events than in the positive set-up events.

Table 4. Descriptive statistics for positive and negative event durations in hours with a plot representing greatest durations in hours by month.

	Positive Event (hrs)	Negative Event (hrs)	All Event (hrs)
Maximum	88	121	-
Mean	51.4	59.3	55.5
Standard Deviation	15.8	25.1	21.3

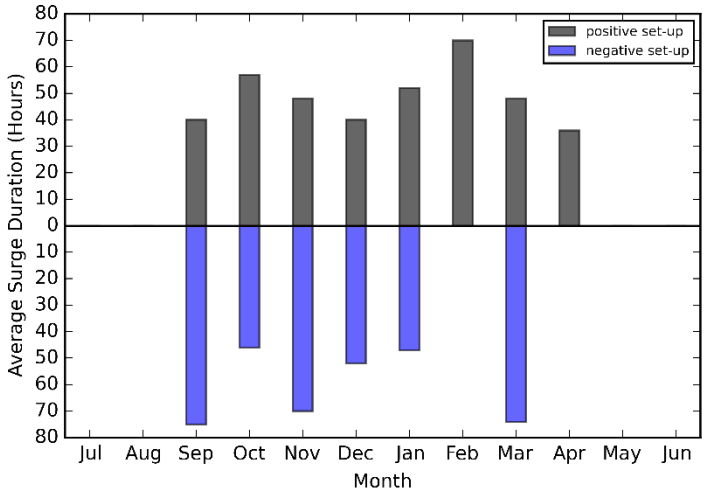

2.4.4. Surge event classifications

The events are classified into four distinct types, labelled A through D (Table 5). Each type is defined by the average onset/peak/return duration of the events within the group. The classification scheme groups both positive and negative set-ups into the same types as their temporal forms are alike.

Table 5. Surge event type classification duration, count, and proportion of the total count.

Category	Average Duration to Peak (h)	Peak Duration (h)	Average Duration form Peak (h)	Total Duration (h)	Count (Σ44)	Proportion
A	24	-	24	48	20	0.45
B	24	-	42	66	10	0.23
C	20	20	20	60	11	0.25
D	60	-	30	90	3	0.07

2.4.4.1. Positive event types: characteristics

The 21 positive set-up events were grouped by temporal evolution; this process resulted in four major types, A through D. A positive Type A event exhibits a rapid onset, approximately 24 hours, to a short-lived peak magnitude and returns to astronomical tide at a rate similar to onset. A positive Type B event exhibits a similar rapid onset and short peak to a Type A, but then returns

to astronomical tide at a gradual rate; approximately twice the duration of the onset. A Type C event exhibits a more rapid onset than type A or B, around 20 hours, and unlike any other type, possesses a long-duration at peak magnitude (15 – 48 hours) before returning to astronomical tide at a rapid rate, similar to its onset. A Type D positive event exhibits a gradual onset lasting 48 hours or more, a short lived peak magnitude, and then a more rapid return to astronomical tide (approximately twice the rate of onset). An example of each event type is reviewed below, along with the synoptic pressure conditions associated with the event

2.4.4.1.1 Example positive Type A event: January 19-21, 2008

An example of a positive Type A event occurred January 19-21, 2008 (Fig. 8). The rising limb duration occurred over approximately 30 hours up to a peak threshold of 1.47 meters, followed by a falling limb duration of approximately 36 hours down to normal astronomical tide level.

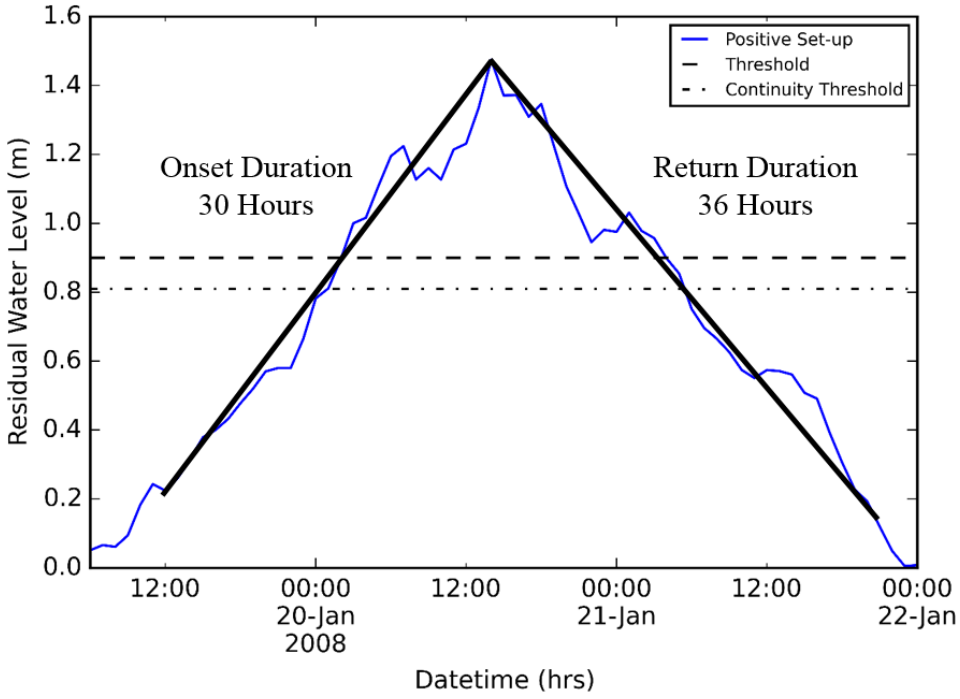

Figure 8. January 19-22, 2008 Type A positive set-up surge event observed at Red Dog Dock, Alaska. The solid black line represents a qualitative best fit delineation of the duration characteristics of the surge onset, peak, and return

On January 19, 24 hours before the water level began rising at Red Dog Dock, a low pressure system entered the southern Bering Sea, midway along the Aleutian Islands. Over the next 24 hours the storm system moved rapidly northward (average track speed of 50km/h). As the storm reached St. Lawrence Island (Fig. 9a) the water level began rising at Red Dog Dock. The storm continued rapidly moving north, crossed the Gulf of Anadyr and the Chukotka Peninsula and moved into the western Chukchi Sea (Fig. 9b), at which point the maximum water level (1.47 meters) was observed. The rapid northward progression continued; 24 hours after peak water level the storm was situated 1000km north of the Bering Strait (Fig. 9c). Water levels began declining immediately after the peak. The rate of water level decrease was similar to the rate of increase, and water levels returned to normal approximately 36 hours after peak.

A
(+)

(a) 24 hours prior

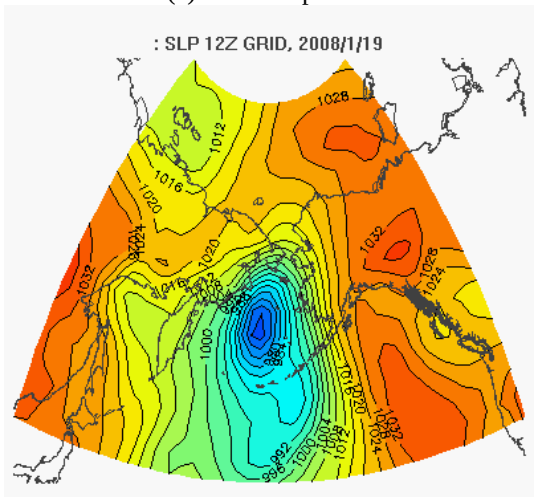

(b) Peak (1.47 m)

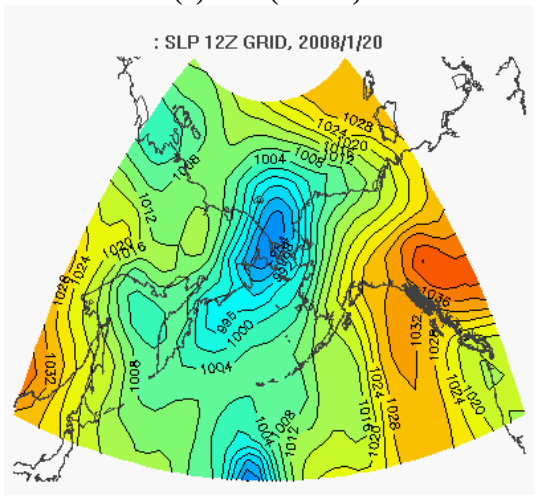

(c) 24 hours after

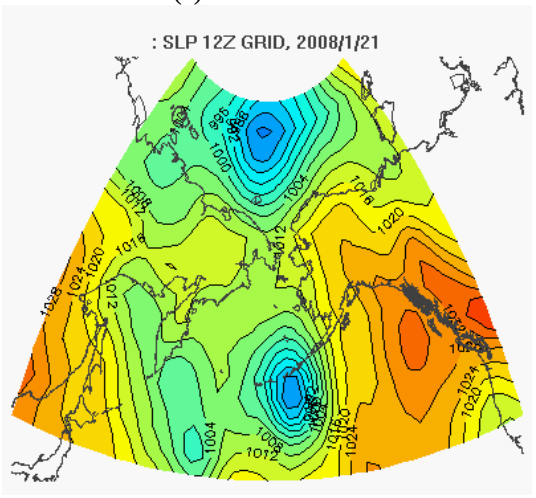

Figure 9. January 19 – 21, 2008 Type A positive set-up surge observed at Red Dog Dock, Alaska. NCEP/NCAR Reanalysis 1 Sea Level Pressure (hPa) before, during, and after peak surge. (a) SLP composite at 12z 01/19 – 24 hours prior to peak magnitude. (b) SLP composite at 12z 01/20 – peak magnitude (1.47 m). (c) SLP composite at 12z 01/21 – 24 hours after peak magnitude.

2.4.4.1.2 Example positive Type B event: October 19-22, 2004

An example of a positive Type B event occurred October 19-22, 2004 (Fig. 10). Water level initially rose rapidly during the first 12 hours and continued to rise less rapidly for an additional 12 hours up to a peak of 1.43 meters. After peak, the water level steadily declined over approximately 48 hours before experiencing a second small rise and continuing (24 hours) its return to normal tide level.

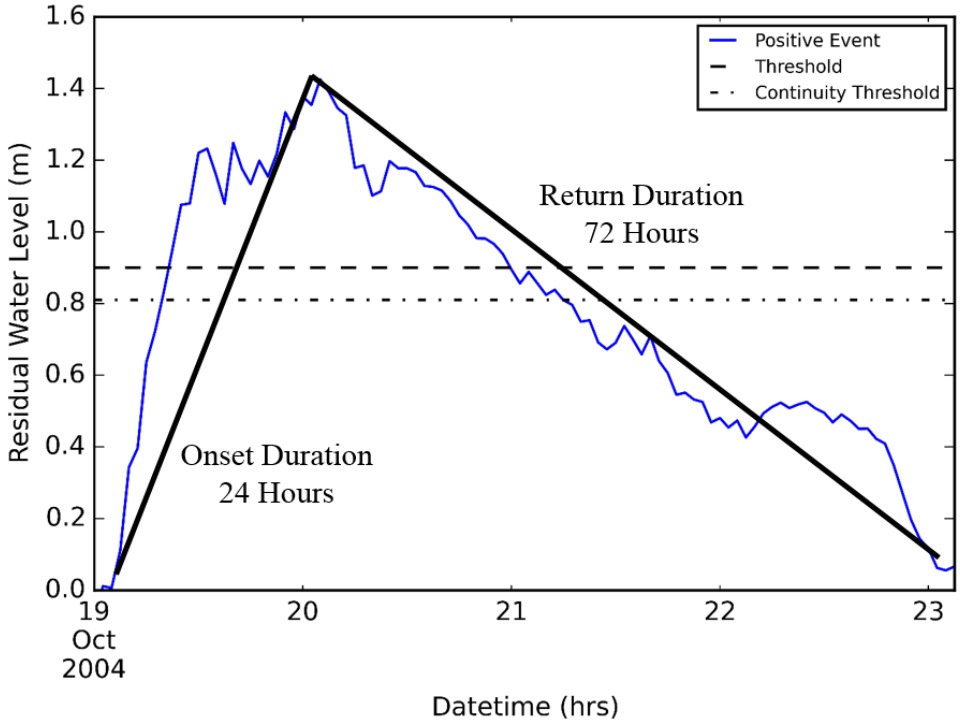

Figure 10. October 19-22, 2004 Type B positive set-up surge event observed at Red Dog Dock, Alaska. The solid black line represents a qualitative best fit delineation of the duration characteristics of the surge onset, peak, and return.

The storm system that drove this event began 72 hours before the onset of rising water levels when a large low pressure system moved into in the western Bering Sea. By October 18 the storm system was rapidly deepening and traveling northeast, following the western coast of the Bering Sea, reaching the Chukotka Peninsula on October 19 with a central pressure in the low 950hPa

range (Fig. 11a). At 00Z on the 19th the water level began its very rapid initial 12 hour rise. Over the next 24 hours the storm system stalled and developed a trough elongation extending over the Chukotka Peninsula (Fig. 11b); during this time the rate of water level rise slowed until it reached its peak of 1.43 m. The storm system remained centered over the Chukotka Peninsula for the next 48 hours, gradually weakening, until it began to break apart into discrete low pressure centers (Fig. 11c). The water levels began declining at a rate twice that of the initial rate of increase, taking the next 72 hours to return to astronomical tide.

B
(+)

(a) 24 hours prior

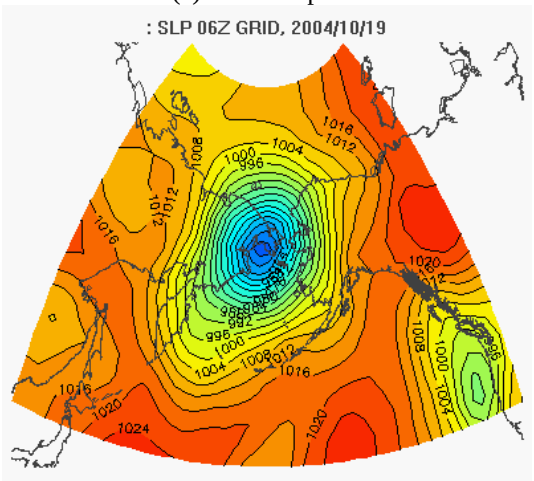

(b) Peak (1.43 m)

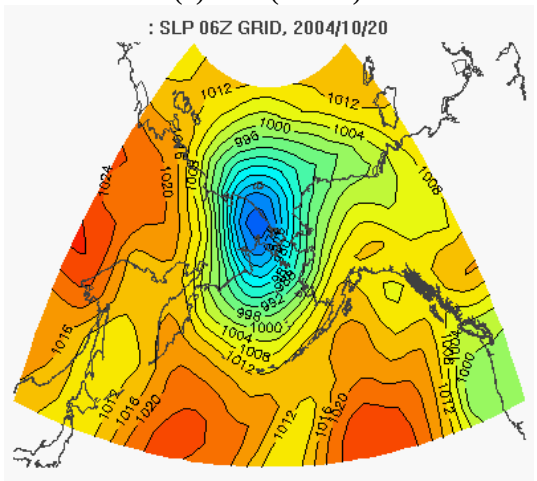

(c) 48 hours after

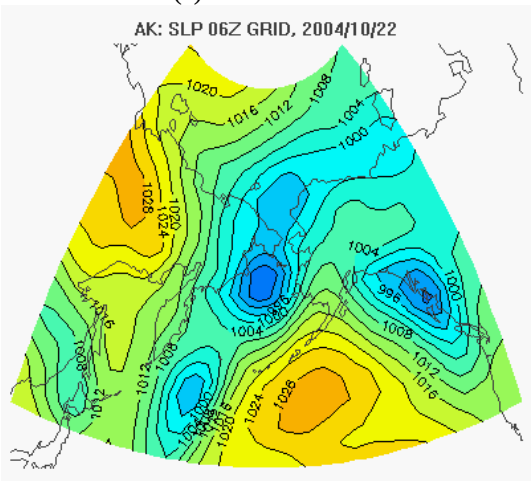

Figure 11. October 19-21, 2004 Type B positive set-up surge at Red Dog Dock, Alaska. NCEP/NCAR Reanalysis 1 Sea Level Pressure (hPa) before, during, and after peak surge. (a) SLP composite at 06z 10/19 – 24 hours prior to peak magnitude. (b) SLP composite at 06z 10/20 – peak magnitude (1.43 m). (c) SLP composite at 06z 10/22 – 48 hours after peak magnitude.

2.4.4.1.3 Example positive Type C event: October 5-8, 2012

An example of a positive Type C event occurred October 5-7, 2012 (Fig. 12). The water level rose over a period of approximately 20 hours, peaked at 1.01 m, remained at this level for approximately 36 hours, and then declined to astronomical tide over a period of approximately 20 hours.

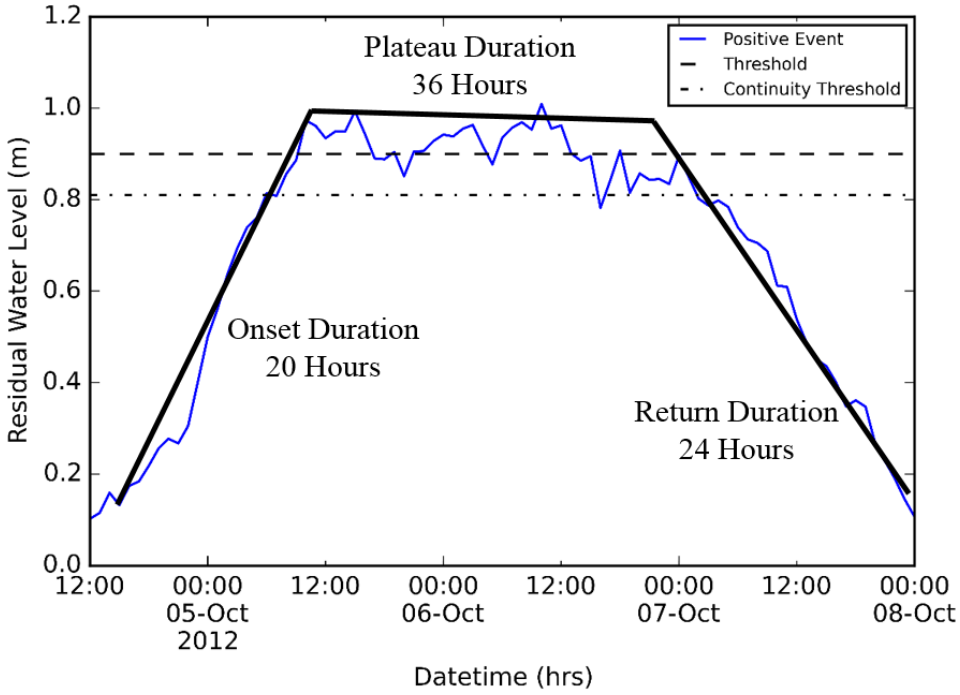

Figure 12. October 5-8, 2012 Type C positive set-up surge event observed at Red Dog Dock, Alaska. The solid black line represents a qualitative best fit delineation of the duration characteristics of the surge onset, peak, and return.

The October 5-8, 2012 surge event began with a low-pressure system that developed off the northeast coast of Japan on October 1. The system tracked northeast, entering the Bering Sea on October 4 from the south, midway along the Aleutian Islands. On October 5 as the system centered over the Bering Sea and began to develop an elongated trough feature to the north and south (Fig. 13a) the water level at Red Dog Dock began to rise rapidly. The system continued to move slowly

northward over the next 30 hours into the Bering Strait (Fig. 13b); during this time the high water levels were maintained. Over the next 30 hours the system moved off to the north and rapidly dissipated (Fig. 13c) allowing the water level to decline back to astronomical over 24 hours.

C
(+)

(a) 30 hours prior

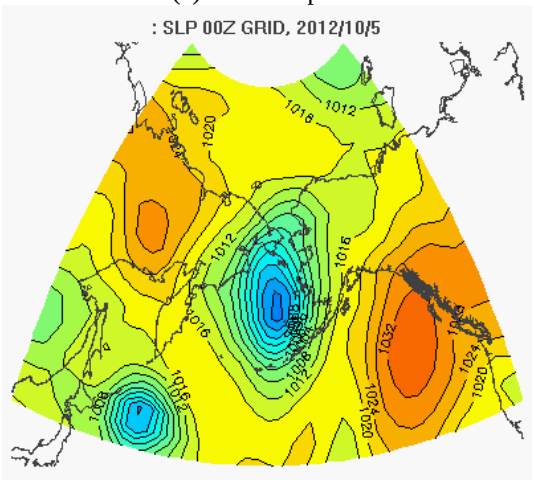

(b) Peak (1.01 m)

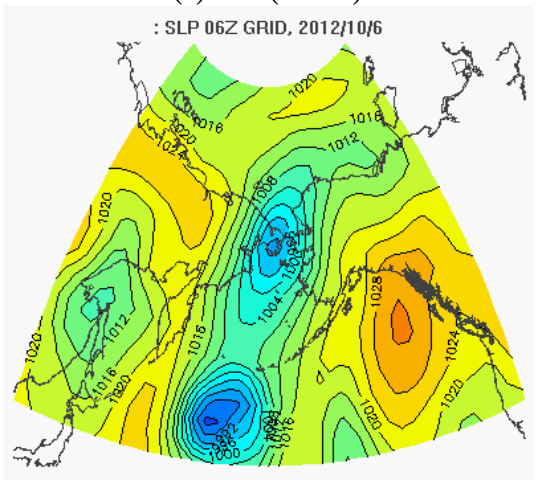

(c) 30 hours after

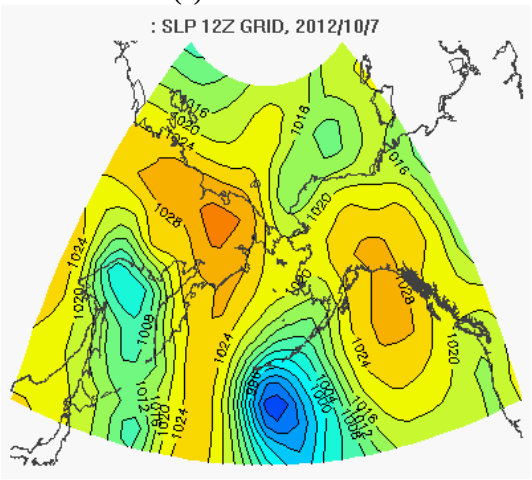

Figure 13. October 5-7, 2012 Type C positive set-up surge at Red Dog Dock, Alaska. NCEP/NCAR Reanalysis 1 Sea Level Pressure (hPa) before, during, and after peak surge. (a) SLP composite at 00z 10/05 – 30 hours prior to peak magnitude. (b) SLP composite at 06z 10/06 – peak magnitude (1.01 m). (c) SLP composite at 12z 10/07 – 30 hours after peak magnitude.

2.4.4.1.4 Example positive Type D event: February 22-26, 2011

An example of a positive Type D surge occurred February 22-26, 2011 (Fig. 14). This event exhibited a slow water level rise beginning late on February 22 and progressing over approximately 48 hours to a peak level of 2.23 meters. After a brief peak duration the water level declines rapidly, over approximately 24 hours, to astronomical tide.

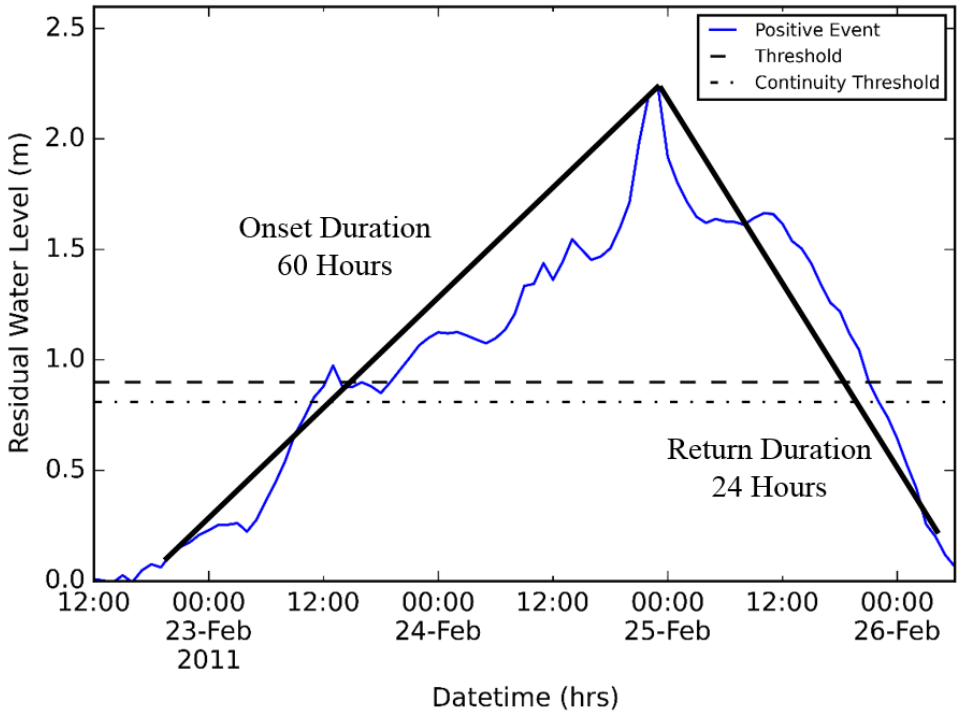

Figure 14. February 22-26, 2011 Type D positive set-up surge event observed at Red Dog Dock, Alaska. The solid black line represents a qualitative best fit delineation of the duration characteristics of the surge onset, peak, and return.

On February 22, 2011, 12 hours before the water level began rising at Red Dog Dock, a developing low pressure system establishes a strong pressure gradient running east-west across the Bering Sea (Fig. 15a). Over the next 12 hours the system rapidly deepens and moves northeast over the Chukotka Peninsula as the water level rises above a meter. The system continues moving northward while a second rapidly moving storm system enters the Bering Sea from the south. As

the second storm system moves in the water level continues to rise over the next 30 hours. At peak water level of 2.23 meters is reached on February 25, the storm is now elongated north-south and centered over the Chukotka Peninsula (Fig. 15b). Next, the storm moves off rapidly replaced by a large high pressure system (Fig. 15c), the water level returns to astronomical tide at a rapid rate.

D
(+)

(a) 60 hours prior

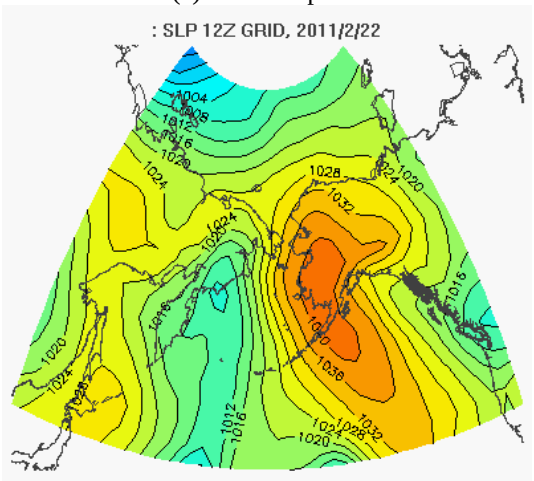

(b) Peak (2.23 m)

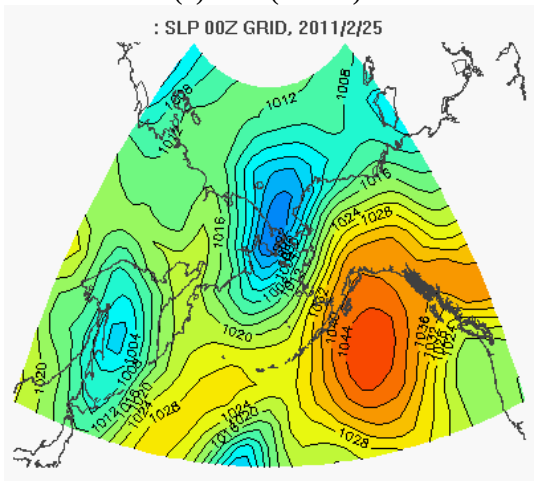

(c) 30 hours after

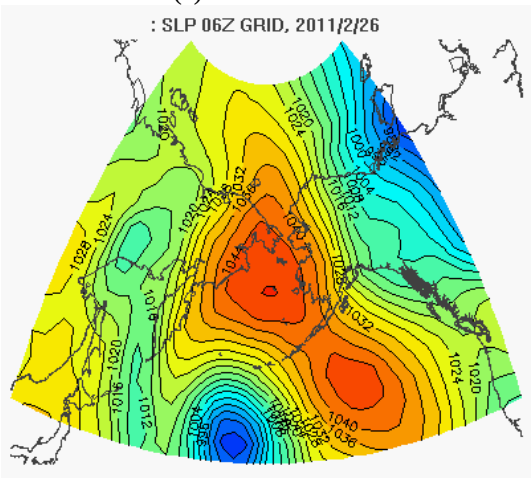

Figure 15. February 22-26, 2012 Type D positive set-up surge at Red Dog Dock, Alaska. NCEP/NCAR Reanalysis 1 Sea Level Pressure (hPa) before, during, and after peak surge. (a) SLP composite at 12z 02/22 – 60 hours prior to peak magnitude. (b) SLP composite at 00z 02/25 – peak magnitude (2.23 m). (c) SLP composite at 06z 02/26 – 30 hours after peak magnitude.

2.4.4.2. Negative event types: characteristics

It was found that negative set-up events could be grouped into four types of similar, but inverse, forms to those that emerged for positive events. Type A negative surge events drop rapidly to peak magnitude, approximately 24 hours, peak briefly and return to normal tide levels at a similar rate. Type B surge events rapidly drop over approximately 24 hours, also pause briefly at peak magnitude and then return to normal tide levels at a more gradual rate, roughly double the rate of onset. A Type C surge event has a more rapid drop than type A or B, around 20 hours, to peak magnitude and maintains a peak level for between 15 – 48 hours before returning to normal tide levels at a similar rate to its onset. A Type D surge event has a gradual onset, 48 hours or more, a short lived peak magnitude, and a rapid (a rate double or greater than the onset) return to astronomical tide.

2.4.4.2.1 Example negative Type A event: December 15-17, 2011

An example of a negative Type A event occurred December 15-17, 2011 (Fig. 16). Similar to a positive Type A event, it is characterized by an almost symmetric form, exhibiting a rapid drop in water level (approx. 24 hrs) to a short-lived peak, followed by an equally rapid return to astronomical tide.

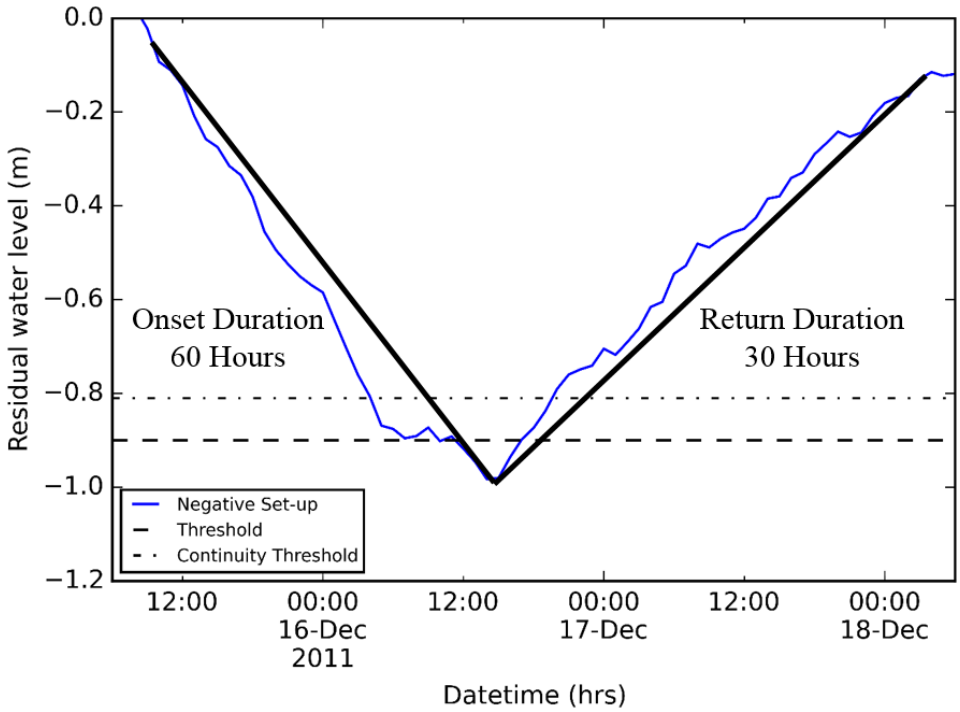

Figure 16. December 15-28, 2011 Type A negative set-up surge event observed at Red Dog Dock, Alaska. The solid black line represents a qualitative best fit delineation of the duration characteristics of the surge onset, peak, and return.

On December 15, 24 hours before the water level began to drop at Red Dog Dock, a low pressure system tracked across the southern Bering Sea to settle over the western tip of the Alaska Peninsula (Fig. 17a) at the point when the storm was at its maximum intensity. Over the next 24 hours leading up to peak surge the storm system remained stationary over the southern Alaska Peninsula (Fig. 17b), slowly declining in strength. After maximum water level (-0.98 m) was reached the storm system developed several deep trough features and continued to dissipate (Fig. 17c); as this occurred over the next 30 hours the water level returned to astronomical tide.

A (-)

(a) 24 hours prior

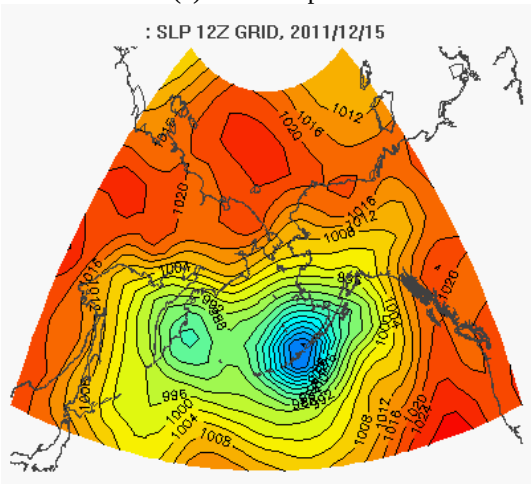

(b) Peak (-0.98 m)

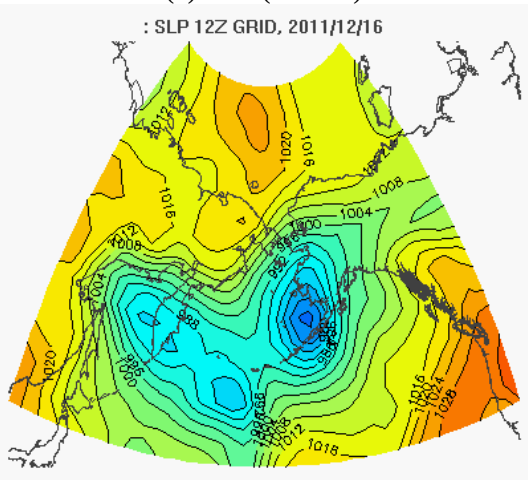

(c) 24 hours after

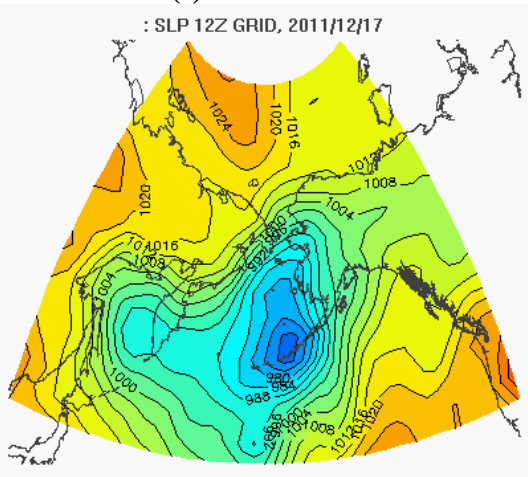

Figure 17. December 15-17, 2011 Type A negative set-up surge at Red Dog Dock, Alaska. NCEP/NCAR Reanalysis 1 Sea Level Pressure (hPa) before, during, and after peak surge. (a) SLP composite at 12z 12/15 – 24 hours prior to peak magnitude. (b) SLP composite at 12z 12/16 – peak magnitude (-0.98 m). (c) SLP composite at 12z 12/17 – 24 hours after peak magnitude.

2.4.4.2.2 Example negative Type B event: December 25-29, 2010

An example of a negative Type B event occurred December 25-29, 2010 (Fig. 18). This negative set-up event exhibited a drop in water level to a magnitude of -1.45 meters over a 36 hour period, after this the water began to rise more gradually, returning to astronomical tide over a period of approximately 72 hours.

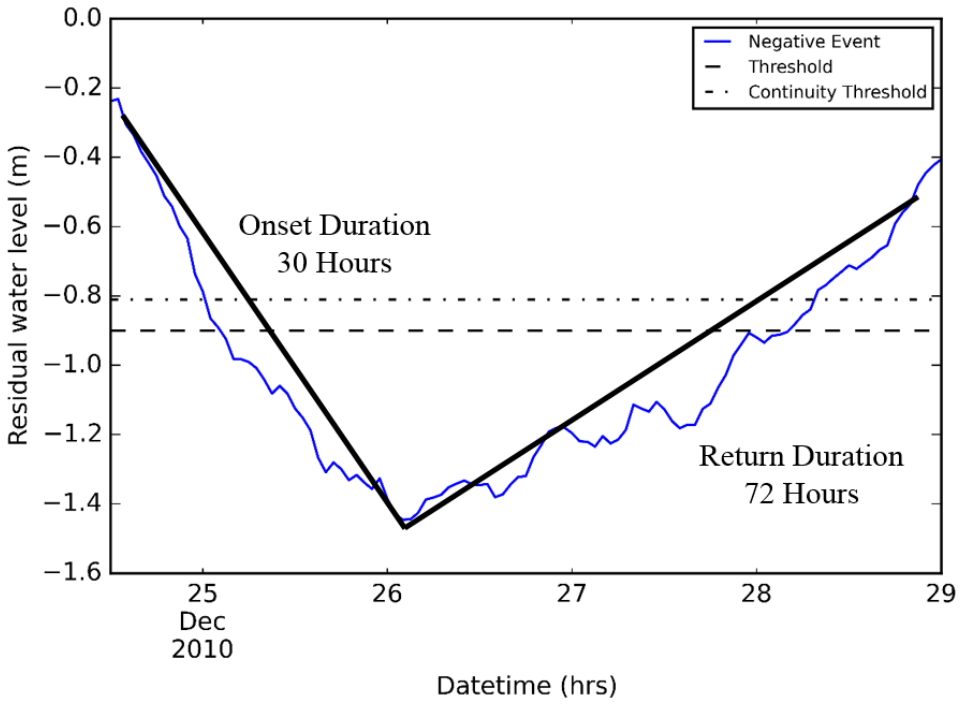

Figure 18. December 25-29, 2010 Type B negative set-up surge event observed at Red Dog Dock, Alaska. The solid black line represents a qualitative best fit delineation of the duration characteristics of the surge onset, peak, and return

This event occurred in response to the pressure gradient set up between an existing strong low in the Gulf of Alaska and a strong high pressure zone over Chukotka Peninsula that built in over the course of the surge event. (Fig. 19a). As the high pressure system strengthened over the next 30 hours the water level dropped to its minimum value of –1.45 m (Fig. 19b). The pressure gradient

weakened in response to a rapid decrease in strength of the Gulf of Alaska low. (Fig. 19c); during this time the water level gradually returned to astronomical tide over a period of 72 hours.

B (-)

(a) 24 hours prior

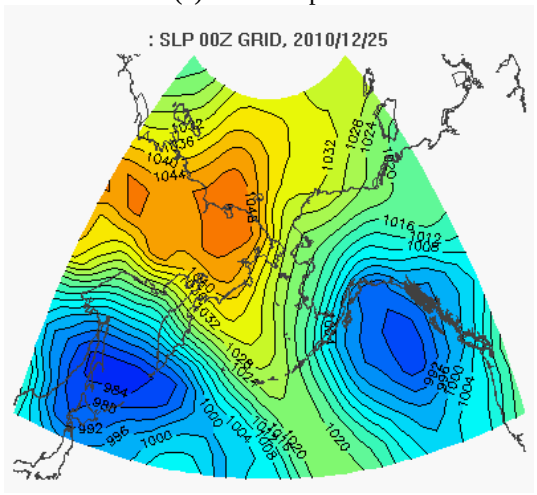

(b) Peak (-1.45 m)

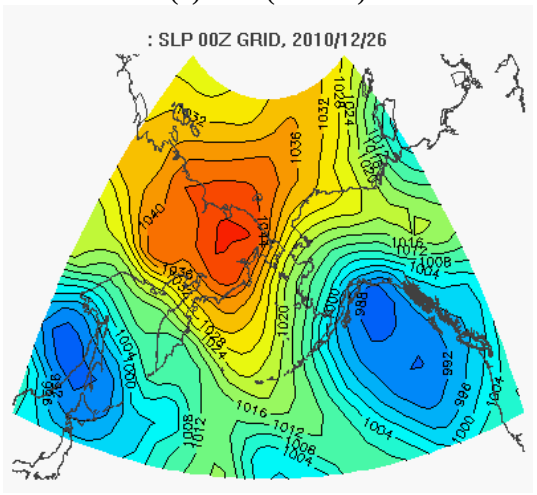

(c) 42 hours after

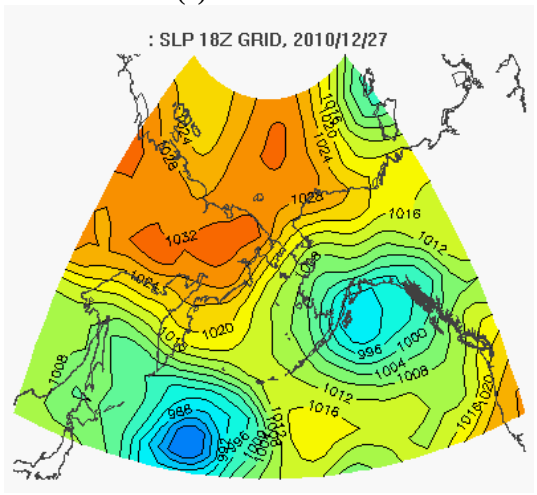

Figure 19. December 25-27, 2010 Type B negative set-up surge at Red Dog Dock, Alaska. NCEP/NCAR Reanalysis 1 Sea Level Pressure (hPa) before, during, and after peak surge. (a) SLP composite at 00z 12/25 – 24 hours prior to peak magnitude. (b) SLP composite at 00z 12/26 – peak magnitude (-1.45 m). (c) SLP composite at 18z 12/27 – 42 hours after peak magnitude.

2.4.4.2.3 Example negative Type C event: November 2-4, 2012

An example of a negative Type C event occurred November 2-4, 2012 (Fig. 20). The water level dropped rapidly over approximately 18 hours, plateaued and remained low for approximately 24 hours, before returning to normal levels (~24 hours).

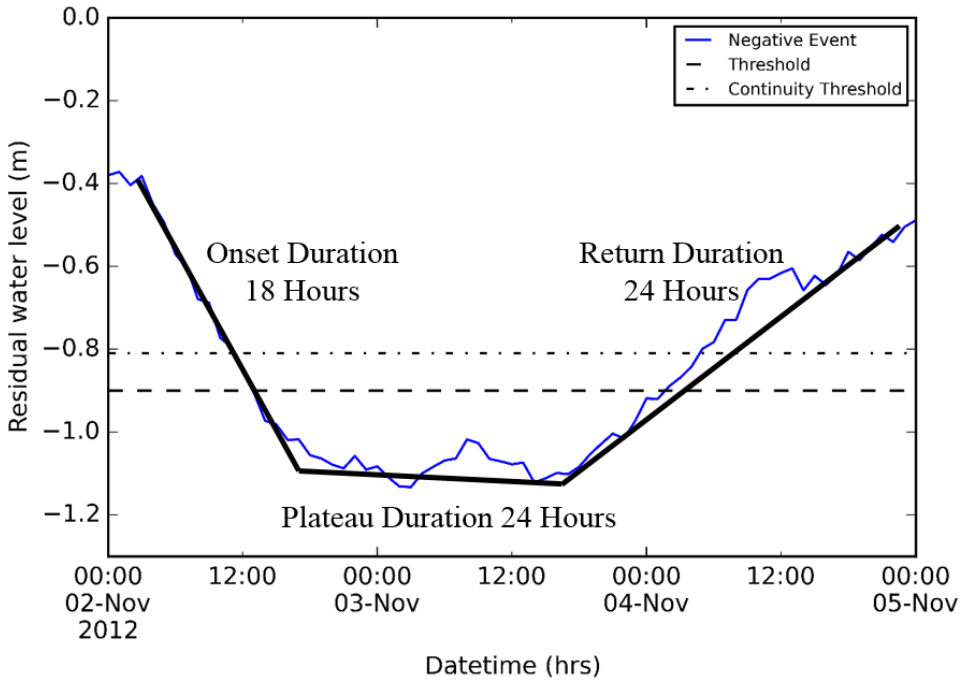

Figure 20. November 2-5, 2012 Type C negative set-up surge event observed at Red Dog Dock, Alaska. The solid black line represents a qualitative best fit delineation of the duration characteristics of the surge onset, peak, and return.

Prior to the drop in water level a very strong low pressure system moved into Gulf of Alaska and stalled (Fig 21a); over the next 18 hours the water level dropped rapidly. The system remained stationary and very slowly weakened over the next 30 hours (Fig. 21b), maintaining a peak water level around -1.13 m. After this the storm system moved off to the south and began dissipating rapidly over the next 24 hours (Fig. 21c); during this time the water level rose at a similar rate to when it dropped, returning to astronomical tide.

C
(-)

(a) 30 hours prior

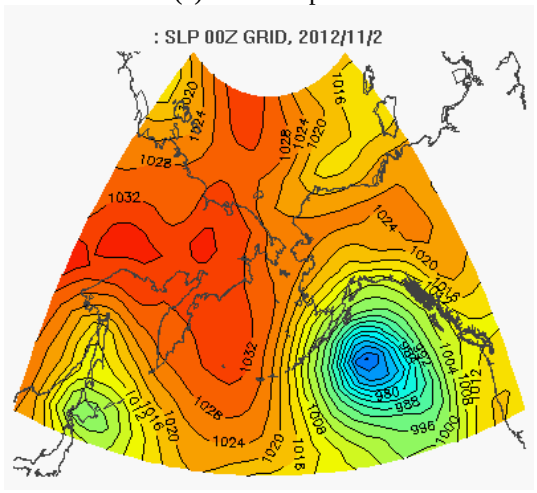

(b) Peak (-1.13 m)

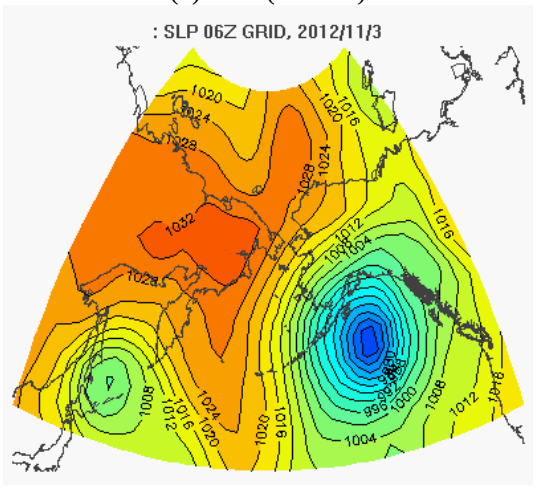

(c) 30 hours after

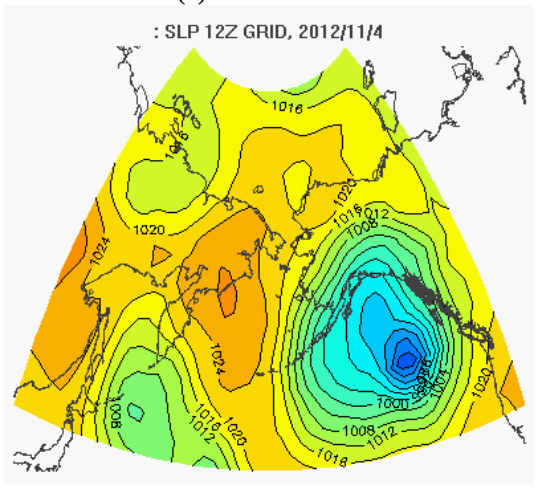

Figure 21. November 2-4, 2012 Type C negative set-up surge at Red Dog Dock, Alaska. NCEP/NCAR Reanalysis 1 Sea Level Pressure (hPa) before, during, and after peak surge. (a) SLP composite at 00z 11/12 – 30 hours prior to peak magnitude. (b) SLP composite at 06z 11/13 – peak magnitude (-1.13 m). (c) SLP composite at 12z 11/14 – 30 hours after peak magnitude.

2.4.4.2.4 Example negative Type D event: November 14-18, 2006

An example of a negative Type D surge event occurred November 17-20, 2005 (Fig. 22). This event exhibited a gradual onset over 48 hours, a short-lived peak magnitude (-1.13 meters), and a rapid return to normal tide levels over 18 hours.

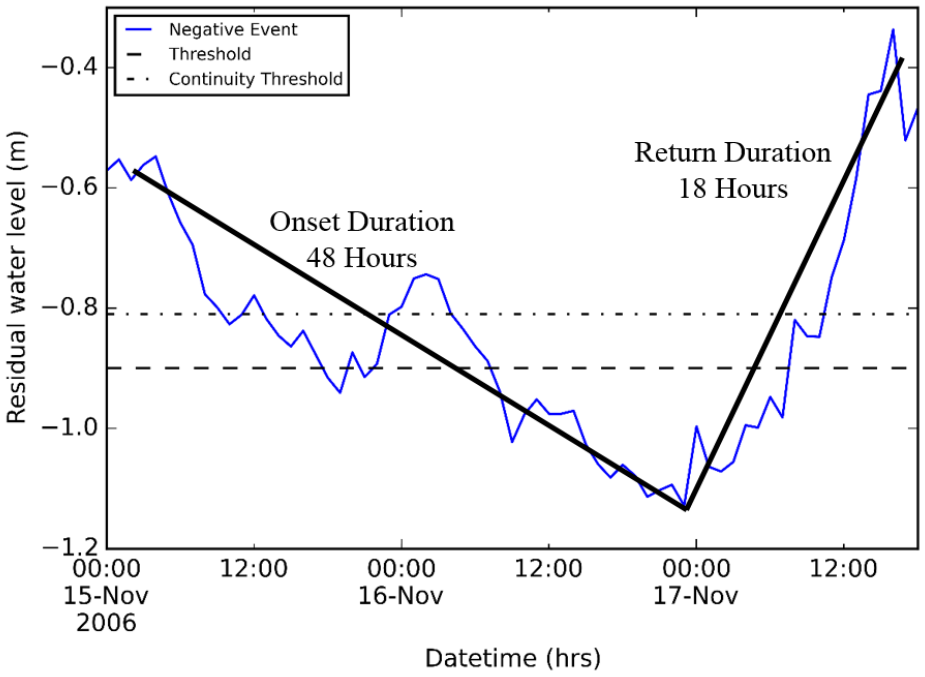

Figure 22. November 14-18, 2006 Type D negative set-up surge event observed at Red Dog Dock, Alaska. The solid black line represents a qualitative best fit delineation of the duration characteristics of the surge onset, peak, and return.

On November 14-18, 2006, 24 hours before the water level began rising a large low pressure system moved into the Gulf of Alaska. Over the next 24 hours the system gained strength while remaining in the Gulf (Fig. 23a). As the water level began to gradually drop over the next 48 hours the storm system entrained a smaller low over Alaska while remaining in the Gulf (Fig. 23b). The pressure gradient over western Alaska changed as a high pressure system strengthened to the north. After a short-lived peak on November 17 the water level increased rapidly back to astronomical

tide over the next 24 hours as the storm system in the Gulf weakened and moved to eastward (Fig. 23c).

D
(-)

(a) 60 hour prior

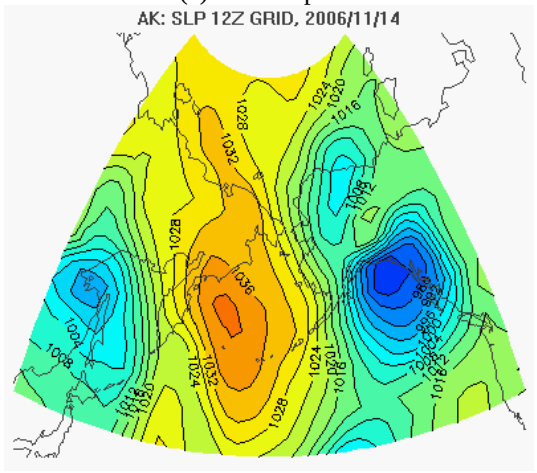

(b) Peak (-1.13 m)

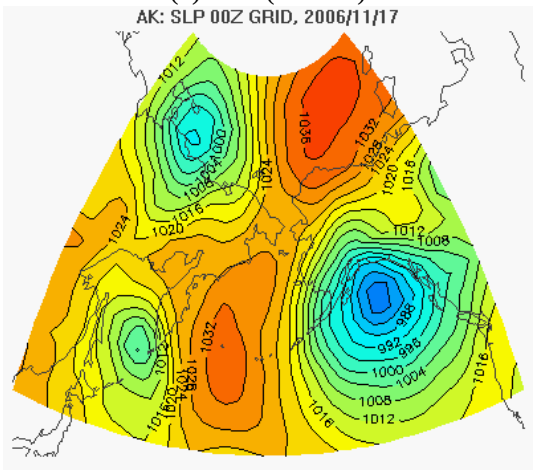

(c) 30 hours after

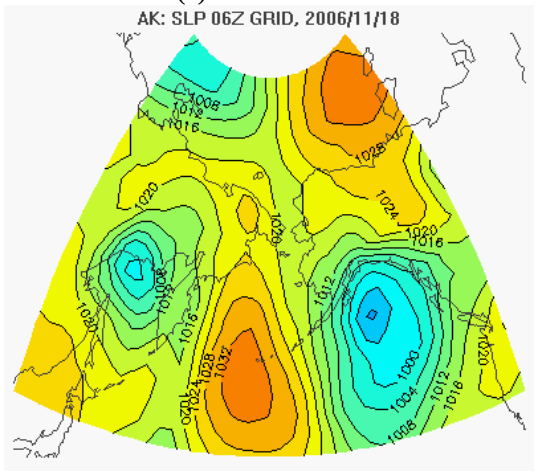

Figure 23. November 14-28, 2006 Type D negative set-up surge at Red Dog Dock, Alaska. NCEP/NCAR Reanalysis 1 Sea Level Pressure (hPa) before, during, and after peak surge. (a) SLP composite at 12z 11/14 – 60 hours prior to peak magnitude. (b) SLP composite at 00z 11/17 – peak magnitude (-1.13 m). (c) SLP composite at 06z 11/18 – 30 hours after peak magnitude.

2.5. Discussion

2.5.1. Identification

Surge events are a direct result of the momentum transfer, or "forcing", generated at the ocean surface by strong atmospheric pressure gradients, usually accompanying low pressure storm systems. These systems are less frequent and of lower intensity in the spring (MAM) and summer months (JJA), than the fall (SON) and winter (DJF) (Mesquita et al., 2010). This explains the basic climatology pattern; that is, that MJJA are devoid of set-up occurrences over the entire 10 year period of analysis. Given that a set-up event depends on transfer of momentum from the moving air to the water, it was interesting to note the months of highest event frequency (NDJ) (Fig. 6) and largest event magnitudes (Table 3) occur when sea-ice is often present throughout the region. Generally, the larger the available open-water fetch the greater the surge response (Squire et al., 2009). Increased sea-ice concentration dampens wave energy, however the influences of the atmosphere on the water column, as it relates to storm surge events, has not been fully explored.

The findings show that large-magnitude positive and negative surge events not only occur during the fall storm season or in open-water conditions, but can occur outside of the fall months and after the sea-ice has set-in. Half of the events recorded at Red Dog Dock occur when sea-ice is present, a time of year that many studies have overlooked as a period with low potential for extreme surge events (Lynch et al., 2008; Manson and Solomon, 2007; Hudak and Young, 2002; Solomon et al., 1994). However, the data have shown here that not only do half of the largest events in the last decade occur during ice-covered periods, but the greatest positive set-up event (2.23 m) occurred when there was more than 1000 kilometres of full sea-ice coverage in all directions.

The ratio of open-water to ice-covered conditions for positive and negative set-up events is 48/52 and 50/50 open-water to ice-covered (Table 6). This is an interesting result, given an expectation for far fewer events to occur under sea-ice conditions than open-water conditions; as the sea-ice acts as both a barrier between the atmosphere and the ocean and has a dampening effect on wave action. It is accepted that sea-ice dampens the meteorological forcing known to generate coastal surge events (Lynch et al., 2008; Atkinson, 2005; Hudak and Young, 2002). Wise, Comiskey, and Becker (1981) discuss surge potential under sea-ice conditions, citing Zubov (1945) and Henry (1975), who describe surge events greater than 3 feet (0.9 metres) measured in ice-covered conditions; and although others (Henry and Heaps, 1976; Blier et al., 1997; Lynch et al., 2008) mention the potential of ice-covered surge events, few studies consider winter (sea-ice) surges to have much potential. However, this study presents compelling evidence indicating an equal or greater potential for large magnitude surge events occurring outside of the commonly accepted periods of greatest potential (i.e., open-water season), at least for this region.

Table 6. Ratio table describing the proportion of event sea-ice coverage.

	Open-water	Ice-covered	Sum
Positive surge	0.24	0.24	0.48
Negative surge	0.26	0.26	0.52
Sum	0.50	0.50	1.00

2.5.2. Classification

Collectively all of the observed surge events follow a similar temporal pattern; as a strong storm system enters the region and establishes a favorable pressure gradient and wind field, a water response commences. This grows as the storm system intensifies and moves through the region until a peak water level response is reached. As the storm system weakens or moves out of the region the observed water level returns to normal.

There are several synoptic patterns that can be matched to each of the temporal surge set-up types, as outlined above. The most common surge event (Type A) resulted from a strong low pressure system tracking north over the Bering Sea, resulting in a rapidly rising positive set-up. However, a negative Type A set-up is the result of a low pressure system rapidly tracking along the Aleutian Islands into Bristol Bay (SE Bering Sea) or the northern Gulf of Alaska.

The Type D pattern was the least numerous and most varied in its temporal set-up for both negative and positive events. However, it does contain the largest magnitude positive and negative set-up surge event observed at Red Dog Dock over the period 2004-2014. It is clear when interpreting the temporal water level pattern and the synoptic circulation patterns for these two events that they experienced multiple storm systems in short succession to generate the observed water levels. Knowing the synoptic patterns associated with Type D events is likely of particular interest to forecasters because they are uncommon, yet high magnitude and potential impact.

2.6. Conclusion

This paper established a surge event identification algorithm and applied it to a continuous time series of water level data at Red Dog Dock, Alaska that has not been subjected to study. The resultant database has established a baseline of surge activity in the area, with frequency analyses developed around surge set-up type (either positive or negative), season (month), sea-ice condition (present/not present), duration, and magnitude. This work identified the most active time of year as the late fall and early winter (November, December, and January), a period of frequent storm incursion into this region. The findings in this study demonstrate that there is equal potential for open-water surge events as there is for ice-covered surge events in the region. This is true for both positive and negative set-up events presenting unexpected finding.

The duration of a negative and positive set-up event is similar, negative events tend to have a slightly greater average duration overall than positive events. The storm systems associated with negative set-up events are often long lived and stationary, whereas storms associated with positive set-up events are often short lived, move rapidly through the region, and occasionally occur in short succession.

In addition the categorization of surge events into similar types based on duration provided two key insights. Firstly, Type A events are the most frequent surge type to occur, exhibiting the lowest variability in form. Secondly, Type D surge events occur the least frequently, but with the greatest magnitude and variability in their form.

3. Evaluating the relationship between synoptic sea level pressure weather patterns and surge events using empirical orthogonal function analysis

3.1. Abstract

The North Bering - South Chukchi Sea region has an active storm season that can generate well-developed wave states and drive positive and negative water level set-up conditions in coastal areas. The northwestern coastline of Alaska is regularly impacted by storms. The low coastal relief and unconsolidated sediments of the region make it particularly vulnerable to coastal erosion and flooding. A database of positive and negative set-up events has been established using a ten year record (2004-2014) of data from a NOAA water level station located at Red Dog Dock on the northwestern coast of Alaska. This surge event database is used here to guide the selection of atmospheric surface pressure data (SLP) which were then reduced using an Empirical Orthogonal Function (EOF) analysis to identify principal patterns associated with surge events. The first two EOFs explained more than 50% of the total variance. EOF 1 was found to represent a positive surge event pattern, consisting of a low pressure system with a roughly north-south elongation situated over the Chukotka Peninsula and western Bering Sea. EOF 2 was found to represent a negative surge event pattern, consisting of a broad low pressure system situated over the eastern Aleutian Islands – the familiar Aleutian Low Pattern. Additional results indicated that negative surge response magnitudes were correlated with duration of the favourable pressure pattern, however this was not observed with positive events. The likely reason for this is the directional forcing required to generate the necessary fetch to drive a positive set-up surge is highly constrained due to the juxtaposition of the Seward Peninsula to the south of Red Dog Dock. This means that, even for a powerful storm, the window of opportunity for surge generation is limited.

This is less the case for a negative surge; any strong wind from the landward side will generate a surge response, a condition that is more readily attained and maintained.

3.2. Introduction

Coastal regions in western and northern Alaska are subjected to temporary changes in water level that are up to four days in duration. These events are termed positive or negative wind set up events, also known as storm surges. Surges are caused when persistent winds are able to entrain the uppermost several meters of the water column, via transfer of momentum, and drive it towards or away from the shore. Winds of sufficient strength to do this are associated with specific patterns of atmospheric pressure; storms in particular or other situations that result in the establishment of strong pressure gradients (Trigo and Davies, 2002). Surge magnitude is locally moderated by nearshore bathymetry and coastal morphology. Surges of particularly large magnitudes (3+ m) have been recorded along the Bering and Chukchi Sea coasts of Alaska (Fathauer, 1997). This in turn can cause physical impacts along the coastal zone, such as inland salt-water flooding, episodic erosion, and damage to community and industry infrastructure (Lantuit et al., 2012; Mason et al., 2012).

To better understand the atmospheric driving mechanisms of storm surges in western Alaska it is useful to look for commonalities in pressure patterns. Empirical Orthogonal Function (EOF) analysis, described in detail below, is used here to perform this grouping. A database of surge events has been compiled using data from a NOAA water level station record at Red Dog Dock on the northwest coast of Alaska (Fig. 1). An EOF is then applied to mean sea level pressure data (described below) for the time periods of interest as defined by the surge events. The ultimate goal of this paper is to isolate major patterns relating broad (synoptic) scale atmospheric circulation patterns to extreme coastal surge events in the North Bering – South Chukchi Sea region.

3.3. Methods

3.3.1. Data

Coastal surge events are defined to be abnormally high/low residual water levels, measured as the difference between observed water level and predicted astronomical tide level (Blier et al., 1997). The water level data used here for analysing coastal surge events were acquired from NOAA/NOS/CO-OPS (National Oceanic and Atmospheric Administration/National Ocean Services/Center for Operational Oceanographic Products and Services). These data are available at hourly intervals since July 2004 at Red Dog Dock, Alaska station 9491094. Observed water levels based off the Red Dog Dock station 9491094 datum (0.00 meters) calibrated to the North American Vertical Datum of 1988 (NAVD88) were converted to residual values (verified observed water levels less the expected astronomical tide levels) and used as input data.

The meteorological data used to identify atmospheric forcing in the region was SLP gridded data from the NCEP/NCAR (National Center for Environmental Prediction/National Center for Atmospheric Research) Reanalysis 1 project (Kalnay et al., 1996) provided by the NOAA/OAR/ESRL (Ocean and Atmospheric Research/Earth System Research Laboratory) PSD (Physical Sciences Division), Boulder, Colorado, USA, from their web site at http://www.esrl.noaa.gov/psd/. These data (termed NNR hereafter) are available at six hour intervals since January 1948 at 2.5˚ latitude/longitude resolution globally; the data was constrained to the Bering Sea region at 40˚N to 80˚N and 130˚E to 240˚E.

3.3.2. Empirical orthogonal function

EOF analysis is designed to rearrange variance within the existing vectors of a dataset into a series of new vectors that capture the most prevalent patterns of variance in the dataset.

A data vector within an EOF consists of a series of individual time steps of a variable possessing spatial extent (Wilks, 2011). The use of EOF and allied methods (e.g. Principal Components Analysis) is common in atmospheric sciences, climatology, and many branches of geographical inquiry (e.g. Richman, 1986; Overland et al., 2002; Hannachi et al., 2007; Danielson et al., 2011). EOF use in atmospheric sciences focuses on the analysis of data fields such as, geopotential height, precipitation, or temperature. It is common to utilize EOF analysis to explore, interpret, and express the joint space/time variations contained in these data series (Wilks, 2011).

In general the classification of data requires two primary steps: the definition of classes that are appropriately matched to the data, and the assignment of each instance into the most suitable class (Cassano, et. al., 2011). There are three main classification methods: subjective, objective, and a hybrid approach, which employs a subjective method of initial data selection with an objective or automated method of assignment.

In this work a hybrid approach is employed to relate atmospheric circulation patterns to observed coastal surge events. The subjective aspect consists of selecting sea level pressure data for each surge event. The objective aspect involves use of a mathematical routine – EOF analysis in this case – to extract the most prominent modes of variability within the SLP data. This should identify the most typical pressure patterns associated with the events identified in the storm surge database. The hybrid approach was adopted, rather than a fully objective approach, to identify subtle difference in the pressure patterns directly associated with surge activity. If all SLP data for the 2004-2014 time period were used, as would be the case for a fully objective approach, the pressure pattern signals associated with surges would be overshadowed by more prevalent patterns.

3.3.3. Analysis approach

The observed water level data at Red Dog Dock for the ten year period 2004-2014 have been analysed (Chapter 2) and a database of positive and negative water level set-up events established. This was performed using a heavily modified version of Atkinson's (2005) multi-stage storm identification algorithm applied to residual water level height and duration (see chapter 2 of this document for a full description of the algorithm) obtained from the NOAA water level station at Red Dog Dock.

The events identified in the database were analysed and grouped on the basis of how the events evolved over time; that is, rapid or gradual rise, rapid or gradual descent, brief or long lived peak. This analysis resulted in four types: Type A rapid rise with a brief peak and rapid descent, Type B rapid rise with a brief peak and gradual descent, Type C rapid rise with a long lived peak and rapid descent, Type D gradual rise with a brief peak and rapid descent.

The NNR data were extracted for: 24 hours before and after the Type A (20) surge events, 24 hours before and 42 hours after Type B (10), 30 hours before and after Type C (11), 60 hours before and 30 hours after Type D (3) events identified in the database. This resulted in a set of (44) temporally discrete sets of SLP data (8-15 6 hourly time-steps in each set) over the 2004-2014 period, totalling 425 individual SLP grids. The EOF analysis was run on the subset SLP data and the major functions retained. To better relate the SLP pattern associated with each surge event back to the EOF results, the SLP subset for each event was averaged and compared to the EOFs in order to both interpret the results and to classify each EOF by assigning the individual surge events.

3.4. Results

The EOF analysis generated four dominant patterns – EOF 1,2,3,4 – with the first two patterns accounting for most of the variability. The first two EOF patterns (Fig. 24) explain 56% of the total variance in the surge-event SLP dataset. EOF 1 depicts an elongated low pressure system over the Chukotka Peninsula extending south along the west side of the Bering Sea with a high pressure system east of the Alaska Peninsula. EOF 2 represents a large low pressure system centered over the Aleutian Islands – Bristol Bay that spans the southeast of the region. This is the familiar Aleutian Low pattern (Rodionov et al., 2005; 2007; Pickart et al., 2009). EOF 3 depicts a high pressure system over Alaska with a large low pressure system centred over the Aleutian Islands. EOF 4 has a low pressure corridor stretching from the North Pacific to the Beaufort Sea straddled by two high pressure systems, one centred on the Gulf of Alaska and the other over the Kamchatka Peninsula.

The leading synoptic pattern (EOF 1) represents the positive set-up events, while the second (EOF 2) the negative set-up events. EOF 1 and 2 explain 37% and 19% of the total variance, respectively. EOF 1 represents 19 events, while EOF 2 represents 22 events (Table 7). EOF 3 and 4 represent a much smaller fraction of the positive and negative set-ups. EOF 1 closely matched 19 out of 21 of the positive set-up events, and EOF 2 matched 22 of 23 of the negative set-up events. The surge events that did not match EOF 1 and 2 were a better fit to EOF 3 and 4 (Fig. 25). EOF 3 can be linked to two positive set-up events, while EOF 4 with a single negative set-up event.

Table 7. EOF 1 through 4 – total explained variance – showing a distinction between negative and positive events, and the proportion of total events per EOF.

	Positive Event	Negative Event	Proportion
EOF 1 (37%)	19	-	0.43
EOF 2 (19%)	-	22	0.50
EOF 3 (13%)	2	-	0.05
EOF 4 (7%)	-	1	0.02
	21	23	44 (1)

Composite mean SLP plots (Fig. 26) for each of the surge events were used to match each event to its representative EOF. The four on the left (Fig. 26a) are positive set-up surges, one from each category Type as defined in the previous chapter, and the four on the right (Fig. 26b) are negative set-ups from each category type.

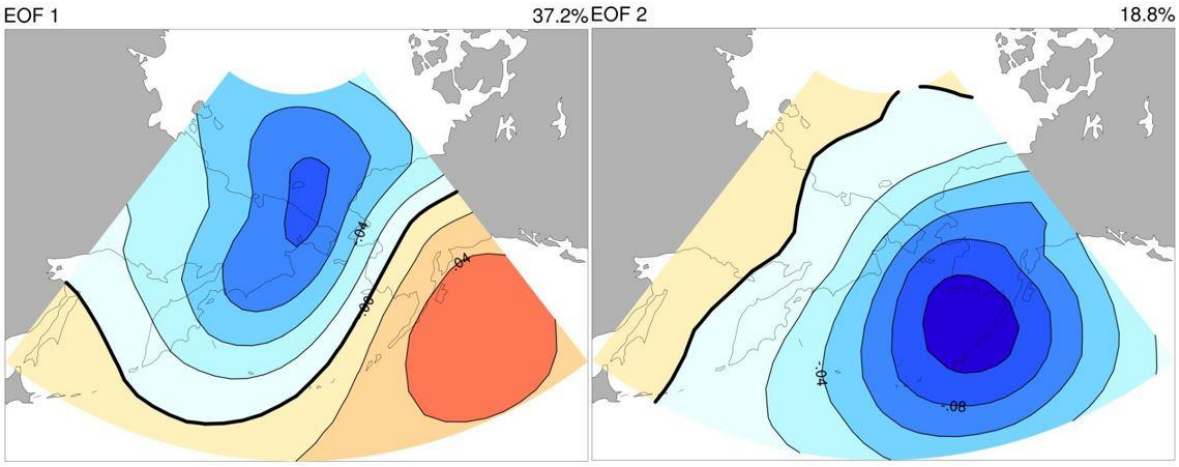

Figure 24. The first and second EOF's for the surge event dataset. Blue shading indicates areas of low pressure and red areas of high pressure. Note winds flow parallel to the isolines of pressure counter clockwise around lows/ clockwise around highs. Geographical domain matches Figure 1.

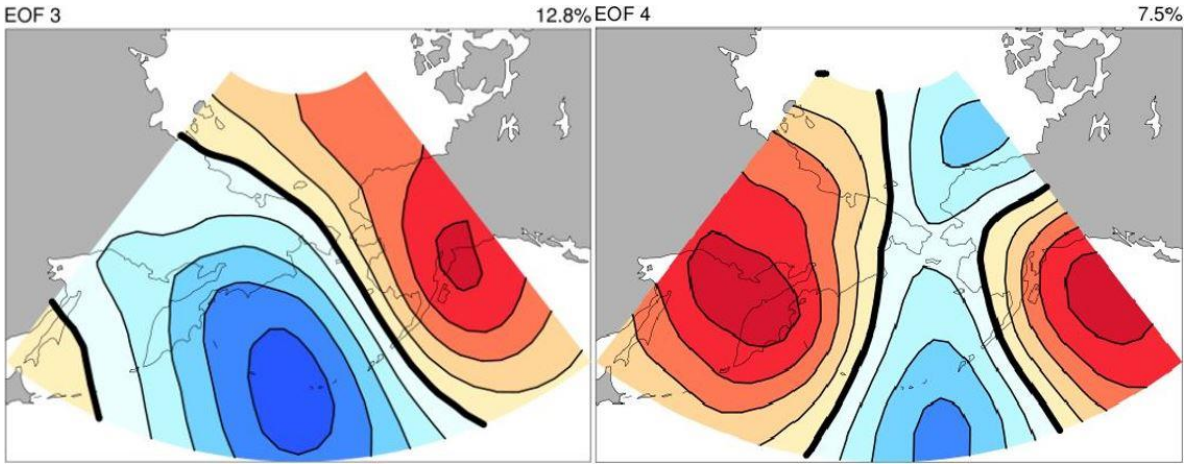

Figure 25. The third and fourth EOFs for the surge event dataset. Blue shading indicates areas of low pressure and red areas of high pressure. Note winds flow parallel to the isolines of pressure counter clockwise around lows/ clockwise around highs. Geographical domain matches Figure 1.

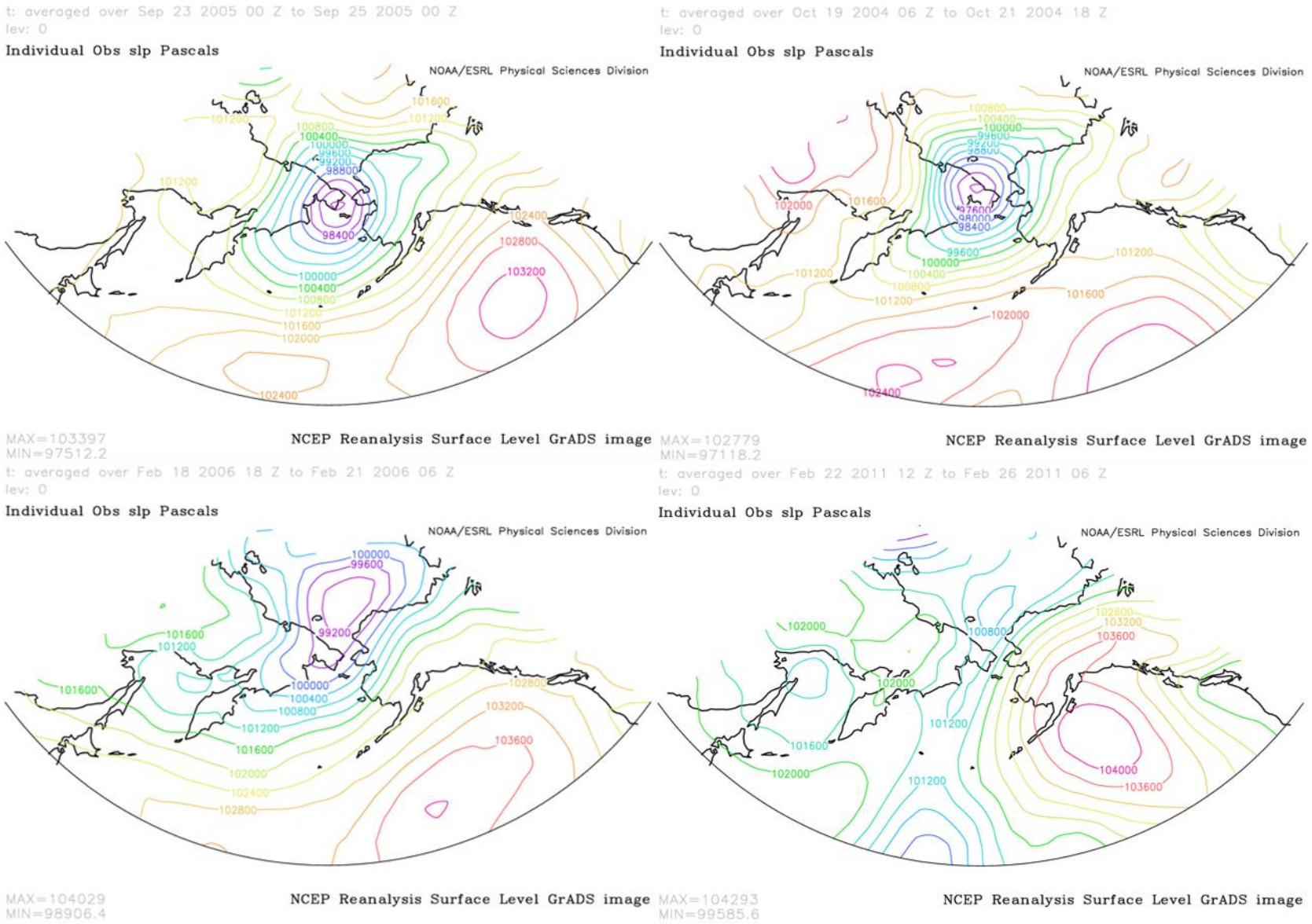

Figure 26. Mean SLP composite examples of positive set-ups for each classification type.

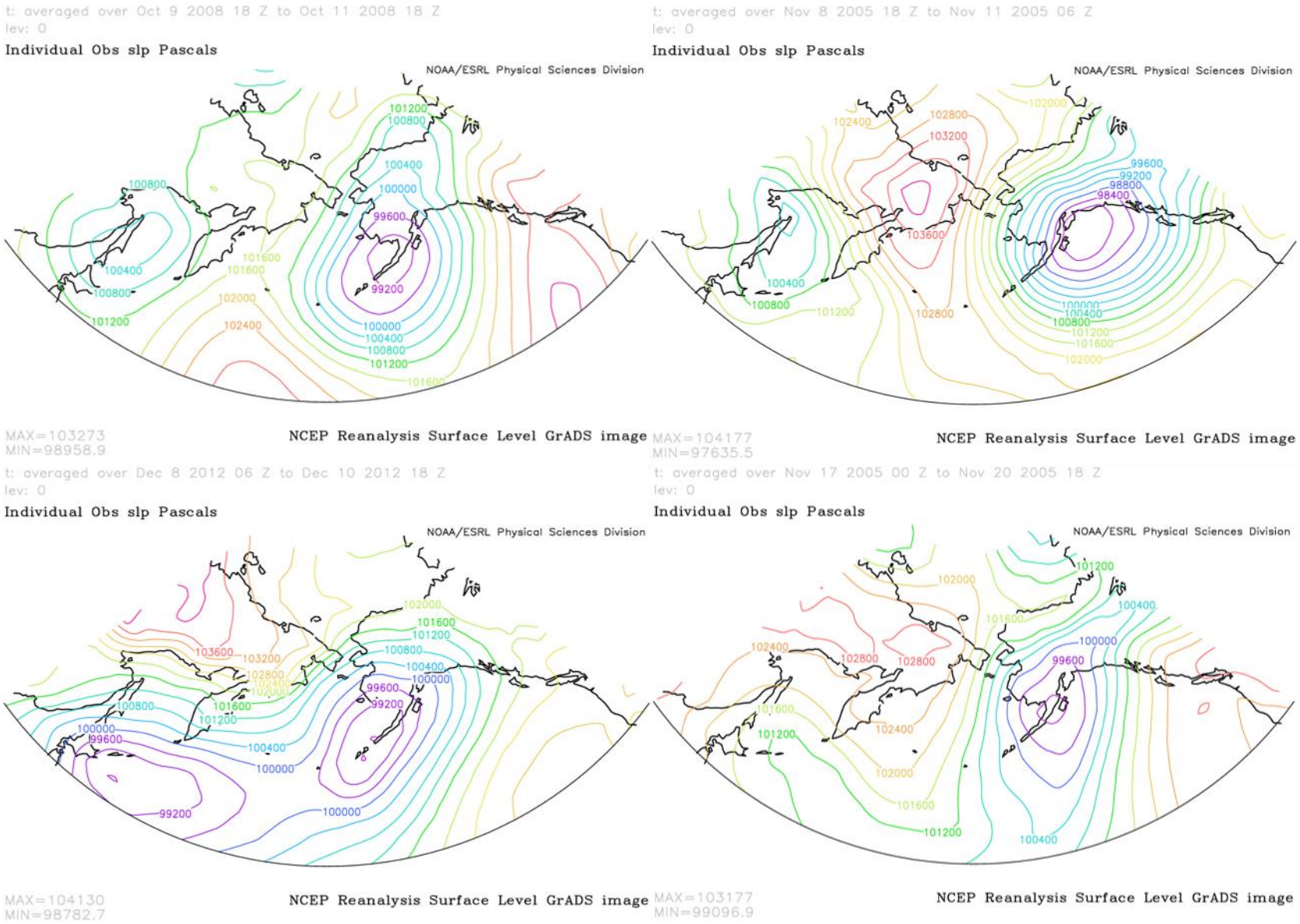

Figure 27. Mean SLP composite examples of negative set-ups for each classification type.

3.5. Discussion

An interesting feature of the EOF analysis emerges when the amount of variance in EOF 1 and 2 is contrasted with the number of events each EOF represents (Table 7): there was an almost equal distribution of events between EOF 1 and 2, however their explained variation is not equal. To address this issue reference is made to the averaged SLP fields for each event, as well as consideration to how EOFs work. Through analysing the event SLP plots a greater variability in negative events is noted, compared to a more consistent pattern among positive set-up events. In particular, the low pressure systems that drive the set up event are positioned over a fairly broad region in southern Alaska, from the central Aleutians over to the eastern Gulf of Alaska. SLP patterns associated with positive SLP events, however, were much more tightly constrained – almost always a low pressure system has to be positioned over the eastern part of the Chukotka Peninsula. The EOF process accumulates variance by looking for pattern similarities; thus, even though there are more negative events, their representative EOF (#2) is an amalgam of a wide range of low pressure systems generally situated south and southeast of Red Dog Dock. EOF 1, however, represents a series of very similar patterns, which pushes up the explained variance value. This helps to explain why, despite the greater occurrence of negative set-ups in the dataset, the positive set-ups still accounts for a greater proportion of the pattern.

Using the EOF results and type classifications it is also possible to evaluate the similarities between the positive and negative set-up events based on event magnitude and duration (Fig. 27). This reveals another difference between the positive and negative set-up events – in the case of a negative surge event the longer the duration of a favorable pressure pattern the larger the surge response. This is not the case for positive surge events.

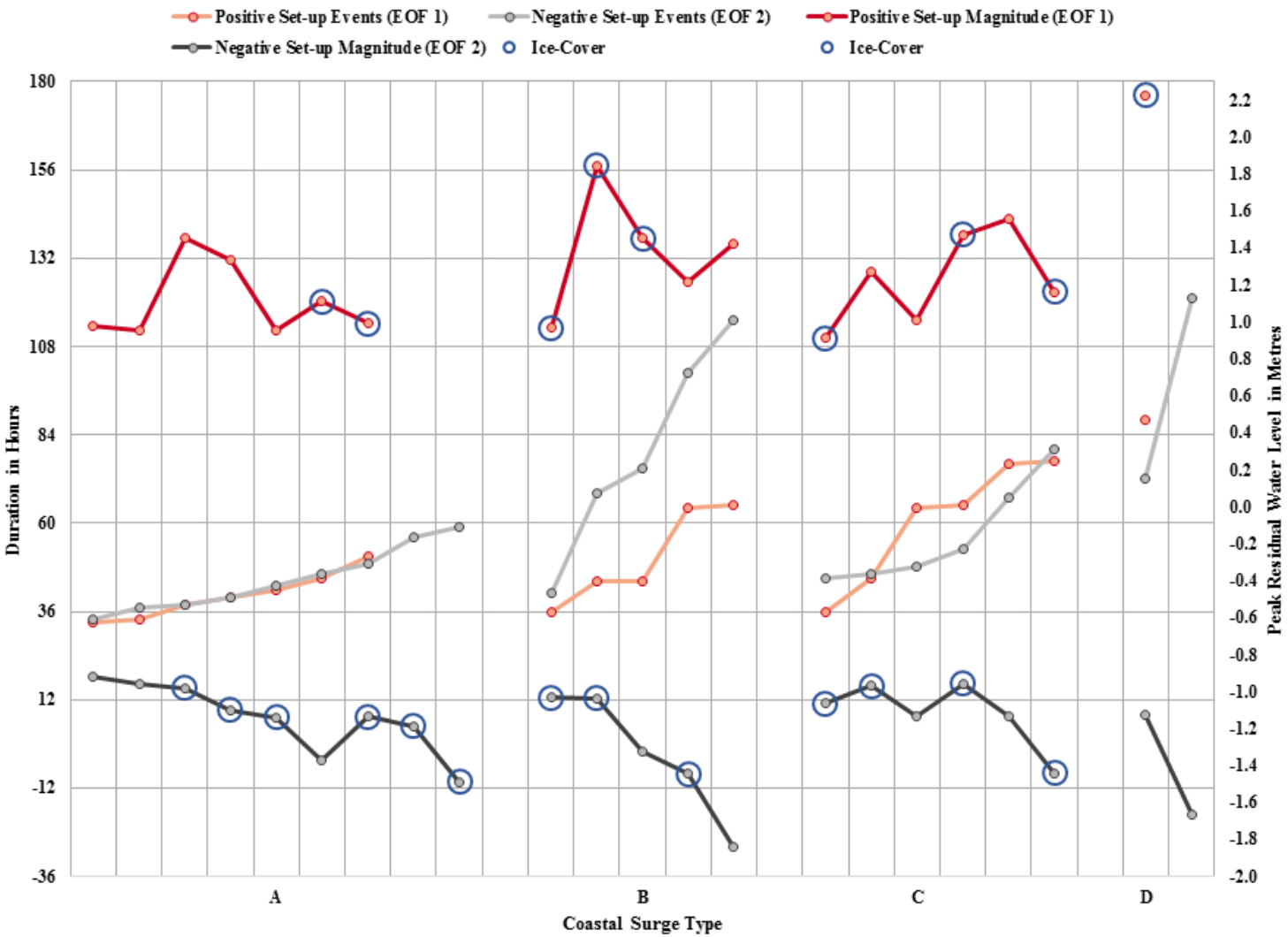

Figure 28. Red line/markers are positive set-up events (EOF 1), grey line/markers are negative set-up events (EOF 2). Left axis is event duration in hours (solid red/grey lines), right axis is event peak residual water level magnitude (faded red/grey lines), and blue circles indicate sea-ice coverage at the time of the event.

Storm systems such as these are identified using an established database of anomalous high/low water levels at Red Dog Dock, Alaska. These identified events are used to define the temporal component for the EOF analysis with gridded SLP reanalysis data. EOF 1 clearly explains the synoptic pattern that results in a positive set-up surge in the region, whereas EOF 2 explains the pattern for a negative set-up coastal surge event.

These findings are verified through the manual comparison of the EOFs to the original SLP data for the period of each event. EOF 1 explains 37% of the variation and EOF 2 19% of the variation, yet EOF 1 accounts for just under half of the events and EOF 2 the other half. This can be explained through analysis of the original SLP patterns; a more limited set-up scenario is required for a positive set-up surge than a negative set-up surge. Even though there are fewer positive set-up events, these events are more similar in their SLP pattern than those of the negative set-up surges. For this reason EOF 1 maintains a greater percentage of the explained variance than EOF 2, despite overall frequency.

It is possible to compare the magnitude and duration of the EOF 1 (positive set-up) and EOF 2 (negative set-up) events when plotted together (Fig. 27). It would appear that the longer a favorable pressure pattern for a negative set-up event (EOF 2) remains in place the larger the surge response tends to be. The same pattern does not persist for positive set-up events (EOF 1), as duration increases magnitude does not necessarily increase. There are two possible explanations for these patterns; either the directional forcing required to favor a positive set-up response is more difficult to sustain than a negative set-up, or there is a much greater sea-ice dampening effect on positive set-up events than negative set-ups.

3.6. Conclusion

The goal of this chapter was to describe the relationship between regional atmospheric circulation patterns and coastal surge events observed at Red Dog Dock. There are additional environmental factors that contribute to both the intensity and magnitude of surge events (such as coastal bathymetry and sea-ice cover), but the primary driving factor is the wind forcing at the surface resulting from pressure gradients, often generated by powerful extra-tropical cyclones (Henry and Heaps, 1976; Mastenbroek et al., 1993; Pirazzoli, 2000; Lynch et al., 2008).

The correlation between duration and magnitude in positive verses negative set-up surge events is an important consideration for future forecasting potential. The greatest risk associated with positive extreme coastal surge events is the risk of inland flooding. Ultimately forecasting can be improved by understanding that prolonged storm duration does not directly correlate to greater magnitude events, rather sea-ice concentration may be a greater contributing factor. However, there are indications that a correlation between duration and magnitude for negative coastal surge events exists. Improved understanding in the forecasting of these events can help to mitigate the potential damages from the break-apart of shore fast ice in strong negative surge events. These findings offer a potential basis for the improved forecasting of both positive and negative set-up events.

4. Concluding remarks

This study examines observational water level data and provides detailed seasonal patterns, overall frequency, and atmospheric driving mechanisms for storm surge events at the Teck Alaska Inc. Red Dog port facility on the southwestern Chukchi Sea coast, Alaska. Positive and negative set-up surge events are identified and classified using a novel algorithm developed for this study. Using this a storm surge event database is built that includes the parameters set-up type (positive or negative), timing, sea-ice concentration, duration, and magnitude. The event database times are in turn used to identify associated atmospheric patterns (sea level pressure). An EOF run on the atmospheric data reduced it to primary patterns that were associated with various set-up events.

Event counts established the most active time of year as the late fall/early winter period (November, December, and January) during open-water and ice-covered conditions when storms are most frequent. An equal number of surge events occurred during ice-covered conditions compared to open-water, for both positive and negative set-ups. In general durations of events of either type are also similar, with negative surge events having slightly longer durations than positive events. Additionally storm systems associated with negative set-up events are often long lived and remain relatively stationary, whereas storms associated with positive set-up events are powerful, short lived, move rapidly through the region, and often occur in multiple succession. Classifying the storm surge events provided two key insights: (1) Type A patterns occur the most frequently and exhibit the lowest variability in set-up form, (2) Type D patterns occur the least frequently, and often have the greatest magnitude and variability in their set-up form.

Ultimately forecasting can be improved through the understanding of storm surge climatology. Knowing that prolonged storm duration does not directly correlate to greater magnitude events, it is rather sea-ice concentration that has a greater potential contributing factor.

Conversely, there appears to be a positive correlation relationship between duration and magnitude for negative surge events. These findings offer the potential for improved forecasting of both positive and negative set-up events in the future.

References

Atkinson, D. E. (2005). Observed storminess patterns and trends in the circum-Arctic coastal regime. Geo-Marine Letters, 25(2-3), 98–109. doi:10.1007/s00367-004-0191-0

Atkinson, D. E., Schweitzer, P., Smith, O., & Norris, L. (2011). The Arctic Coastal System: An Interplay of Components Human, Industrial, and Natural. In Lovecraft, A. L., & Eicken, H. (Eds.), North by 2020 (pp. 81-96). University of Alaska Press.

Bader, J., Mesquita, M. D. S., Hodges, K. I., Keenlyside, N., Østerhus, S., & Miles, M. (2011). A review on Northern Hemisphere sea-ice, storminess and the North Atlantic Oscillation: Observations and projected changes. Atmospheric Research, 101(4), 809–834. doi:10.1016/j.atmosres.2011.04.007

Blier, W., Keefe, S., Shaffer, W. A., & Kim, S. C. (1997). Storm Surges in the Region of Western Alaska. Monthly Weather Review, 125, 3094–3108.

Cassano, E. N., Cassano, J. J., & Nolan, M. (2011). Synoptic weather pattern controls on temperature in Alaska. Journal of Geophysical Research, 116(D11), D11108. doi:10.1029/2010JD015341

Danielson, S., Curchitser, E., Hedstrom, K., Weingartner, T., & Stabeno, P. (2011). On ocean and sea ice modes of variability in the Bering Sea. Journal of Geophysical Research: Oceans, 116(June), 1–24. doi:10.1029/2011JC007389

Fathauer, T. (1997). Wind, Ice, and Sea. In Neal, W. J., & Pilkey, O. H. (Eds.), Living with the Coast of Alaska (pp. 81-96). Duke University Press.

Graham, N. E., & Diaz, H. F. (2001). Evidence for intensification of North Pacific winter cyclones since 1948. Bulletin of the American Meteorological Society, 82, 1869–1893. doi:10.1175/1520-0477(2001)082<1869:EFIONP>2.3.CO;2

Hannachi, a., Jolliffe, I. T., & Stephenson, D. B. (2007). Empirical orthogonal functions and related techniques in atmospheric science: A review. International Journal of Climatology, 27(9), 1119–1152. doi:10.1002/joc.1499

Henry, R. F. (1975). Storm Surges. Beaufort Sea Project, Department of the Environment.

Henry, R. F., & Heaps, N. S. (1976). Storm Surges in the Southern Beaufort Sea. Journal of the Fish Resource Board of Canada, 33(10), 2362–2376.

Hudak, D. R., & Young, J. M. C. (2002). Storm climatology of the Southern Beaufort sea. Atmosphere-Ocean, 40(2), 145–158. doi:10.3137/ao.400205

Johnson, W. R., & Kowalik, Z. (1986). Modeling of Storm Surges in the Bering Sea and Norton Sound. Geophysical Research, 91(April 1986), 5119–5128.

Jorgenson, T., & Ely, C. (2001). Topography and flooding of coastal ecosystems on the Yukon-Kuskokwim Delta, Alaska: implications for sea-level rise. Journal of Coastal Research, 17(1), 124–136. Retrieved from http://www.jstor.org/stable/4300157

Kalnay, E., Kanamitsu, M., Kistler, R., Collins, W., Deaven, D., Gandin, L., … Joseph, D. (1996). The NCEP/NCAR 40-Year Reanalysis Project.

Kowalik, Z. (1984). Storm Surges in the Beaufort and Chukchi Seas. Geophysical Research, 89, 570–578.

Lantuit, H., Overduin, P. P., & Wetterich, S. (2013). Recent Progress Regarding Permafrost Coasts. Permafrost and Periglacial Processes, 24(2), 120–130. doi:10.1002/ppp.1777

Lynch, A. H., Lestak, L. R., Uotila, P., Cassano, E. N., & Xie, L. (2008). A Factorial Analysis of Storm Surge Flooding in Barrow, Alaska. Monthly Weather Review, 136(3), 898–912. doi:10.1175/2007MWR2121.1

Manson, G. K., & Solomon, S. M. (2007). Past and future forcing of Beaufort Sea coastal change. Atmosphere-Ocean, 45(2), 107–122. doi:10.3137/ao.450204

Mason, O. K., Jordan, J., Lestak, L. R., & Manley, W. F. (2012). Narratives of Shoreline Erosion and Protection at Shishmaref, Alaska: The Anecdotal and the Analytical. In J. A. G. Cooper & O. . Pilkey (Eds.), Pitfalls of Shoreline Stabilization: Selected Case Studies (Vol. 3, pp. 73–92). Springer. doi:10.1007/978-94-007-4123-2

Mason, O. K., Salmon, D. K., & Ludwig, S. L. (1996). THE PERIODICITY OF STORM SURGES IN THE BERING SEA FROM 1898 TO 1993 , BASED ON NEWSPAPER ACCOUNTS Coastal dunes and clastic shoreline deposits react rapidly to climate-induced changes (Fox and Davis , 1976), including those associated with the E1 Nifio. Climate Change, 34(1), 109–123.

Mastenbroek, C., Burgers, G., & Janssen, P. (1993). The dynamical coupling of a wave model and a storm surge model through the atmospheric boundary layer. Journal of Physical …, 23, 1856–1866. Retrieved from http://cat.inist.fr/?aModele=afficheN&cpsidt=4855390

McPhee, M. (2008). Air-ice-ocean interaction: turbulent ocean boundary layer exchange processes. Vasa. Retrieved from http://medcontent.metapress.com/index/A65RM03P4874243N.pdf

Mesinger, F., Dimego, G., Kalnay, E., Mitchell, K., Shafran, P. C., Jovic, D., … Shi, W. (2005). North American Regional Reanalysis.

Mesquita, M. D. S., Atkinson, D. E., Simmonds, I., Keay, K., & Gottschatck, J. (2009). New perspectives on the synoptic development of the severe October 1992 Nome storm. Geophysical Research Letters, 36(October 1992), 3–7. doi:10.1029/2009GL038824

Mesquita, M. S., Atkinson, D. E., & Hodges, K. I. (2010). Characteristics and Variability of Storm Tracks in the North Pacific, Bering Sea, and Alaska*. Journal of Climate, 23(2), 294–311. doi:10.1175/2009JCLI3019.1

NANA, Featured Project: Red Dog Mine. (2010). Retrieved December 15, 2014, from http://nana-dev.com/industries/mining/red_dog_mine/

Overland, J. E., Bond, N. a., & Adams, J. M. (2002). The relation of surface forcing of the Bering Sea to large-scale climate patterns. Deep-Sea Research Part II: Topical Studies in Oceanography, 49, 5855–5868. doi:10.1016/S0967-0645(02)00322-3

Pirazzoli, P. A. (2000). Surges, atmospheric pressure and wind change and flooding probability on the Atlantic coast of France. Oceanologica Acta, 23(6), 643–661. doi:10.1016/S0399-1784(00)00122-5

Reimnitz, E. R. K., & Maurer, D. K. (1979). Effects of Storm on the Beaufort Sea Surges Alaska Coast , Northern. Artic Intitute of North America, 32(4), 329–344.

Reynolds, R. W., Smith, T. M., Liu, C., Chelton, D. B., Casey, K. S., & Schlax, M. G. (2007). Daily high-resolution-blended analyses for sea surface temperature. Journal of Climate, 20(1994), 5473–5496. doi:10.1175/2007JCLI1824.1

Richman, M. B. (1986). Review Article: Rotation of Principal Components. Journal of Climatology, 6, 293–335. doi:10.1056/NEJMra1313875

Rodionov, S. N., Overland, J. E., & Bond, N. a. (2005). The Aleutian low and winter climatic conditions in the Bering Sea. Part I: Classification. Journal of Climate, 18(2001), 160–177. doi:10.1175/JCLI3253.1

Simiu, E., & Heckert, N. a. (1996). Extreme Wind Distribution Tails: A "Peaks over Threshold" Approach. Journal of Structural Engineering, 122(5), 539–547. doi:10.1061/(ASCE)0733-9445(1996)122:5(539)

Solomon, S. M., Forbes, D., & Kierstead, B. (1994). Coastal Impacts of Climate Change: Beaufort Sea Erosion Study.

Sprenke, J., Gill, S., Kent, J., & Zieserl, M. (2011). Tides under the Ice : Measuring Water levels at Barrow, Alaska 2008-2010.

Squire, V. A., Vaughan, G. L., & Bennetts, L. G. (2009). Ocean surface wave evolvement in the Arctic Basin. Geophysical Research Letters, 36(22), L22502. doi:10.1029/2009GL040676

Stull, R. B., & Driedonks, A. G. M. (1987). Applications of the transilient turbulence parameterization to atmospheric boundary-layer simulations. Boundary-Layer Meteorology, 40(3), 209-239.

Teck, Red Dog. (2013). Retrieved April 23, 2015, from Teck Alaska Inc. Retrieved April 23, 2015, from http://nana-dev.com/industries/mining/red_dog_mine/

Trigo, I. F., & Davies, T. D. (2002). Meteorological conditions associated with sea surges in Venice: a 40 year climatology. International Journal of Climatology, 22(7), 787–803. doi:10.1002/joc.719

Wadhams, P. (2000). Ice in the Ocean. CRC Press.

Wilks, D. S. (2011). Principal Component (EOF) Analysis. In Statistical Methods in the Atmospheric Sciences (Vol. 100, pp. 519–562). Elsevier. doi:10.1016/B978-0-12-385022-5.00012-9

Wise, J. L., Comiskey, A. L., & Becker, R. J. (1981). Storm Surge Climatology and Forcasting in Alaska.

Zubov, N. N. (1945). Arctic sea ice. Translated from Russian language by Naval Oceanographic Office and American Meteorological Society, 491.

Appendix A

Time series profiles of each individual surge event at Red Dog Dock 2004-2014.

2004 Season

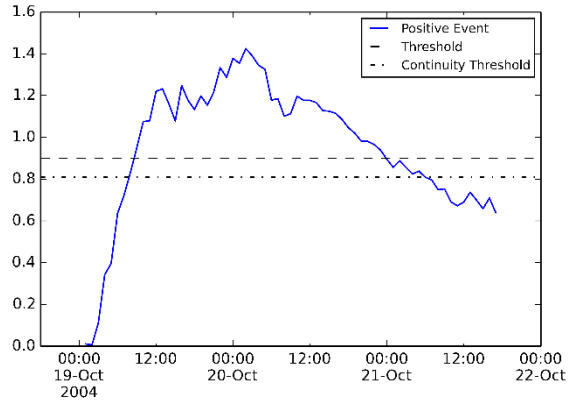

Classification – Type B

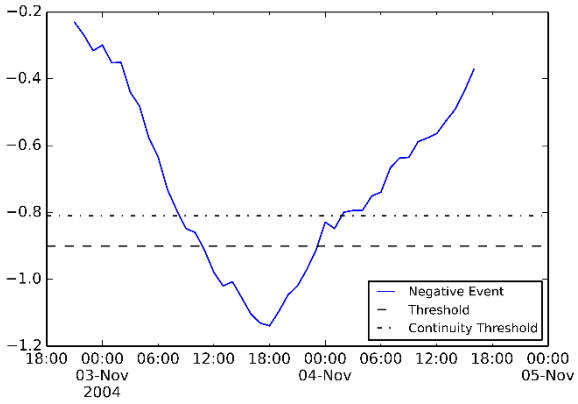

Classification – Type A

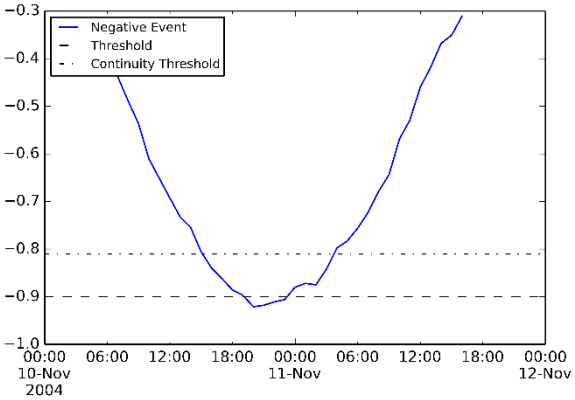

Classification – Type A

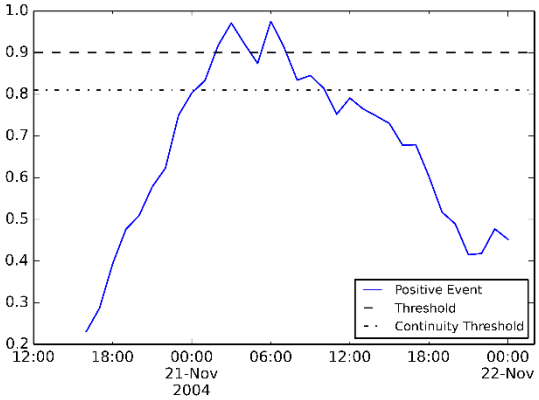

Classification – Type A

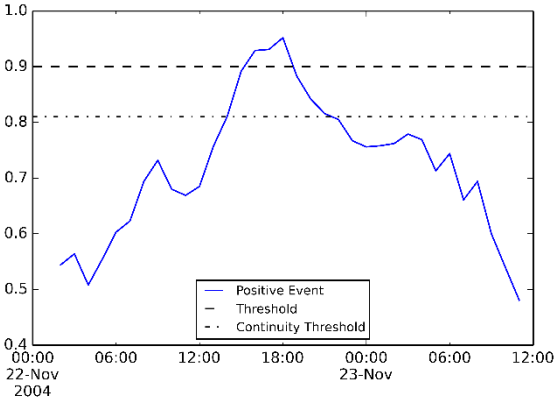

Classification – Type A

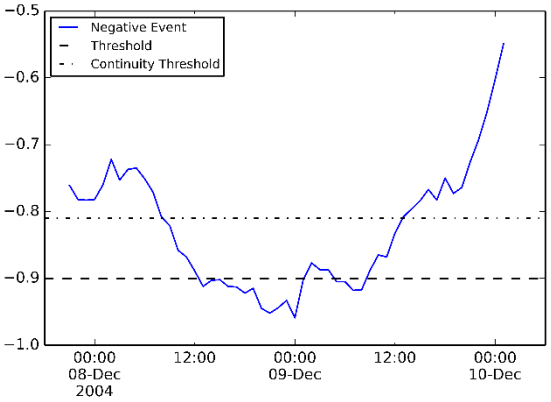

Classification – Type C

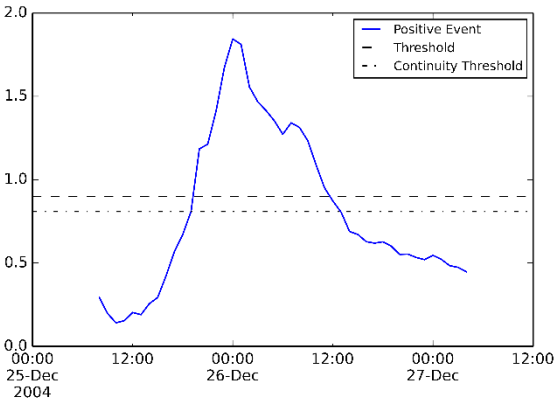

Classification – Type B

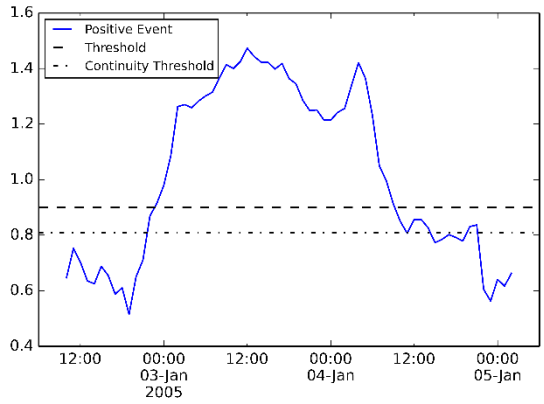

Classification – Type C

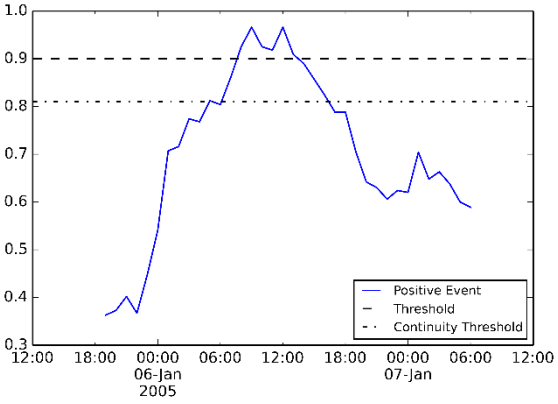

Classification – Type B

2005 Season

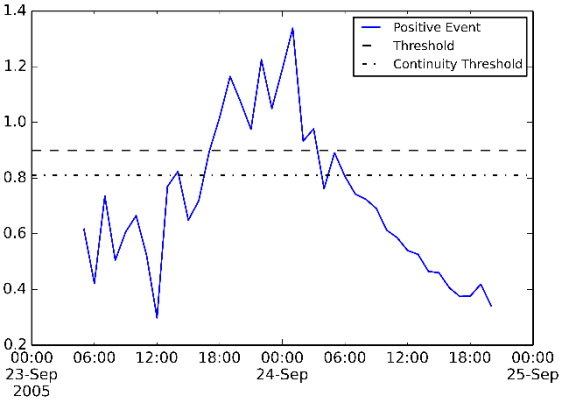

Classification – Type A

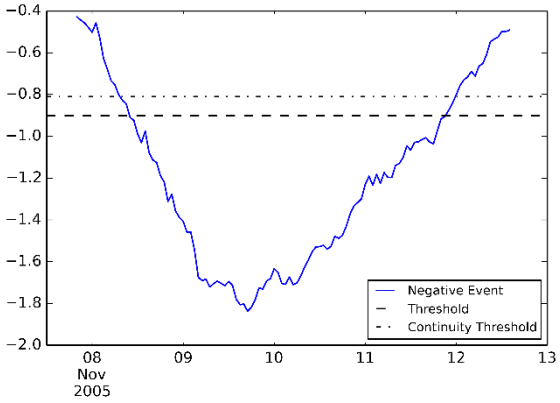

Classification – Type B

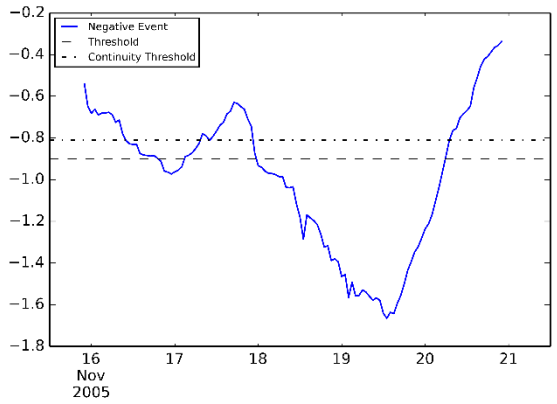

Classification – Type D

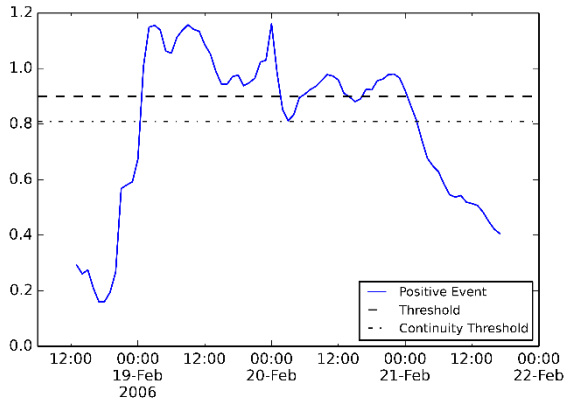

Classification – Type C

2006 Season

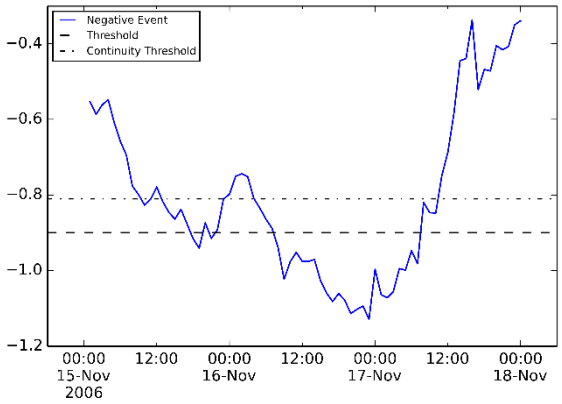

Classification – Type D

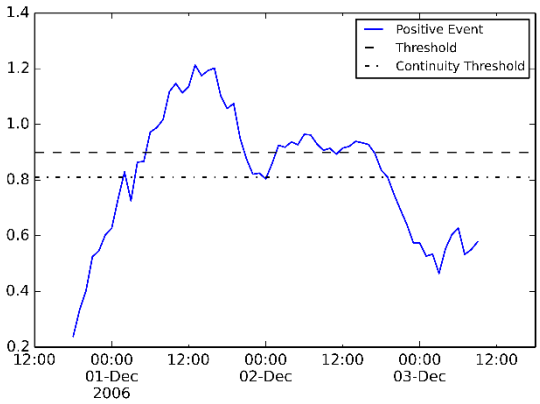

Classification – Type B

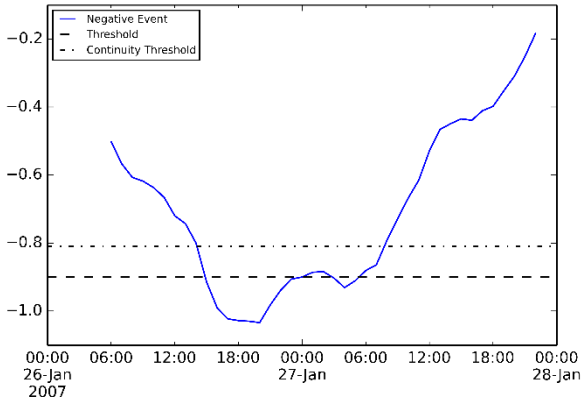

Classification – Type B

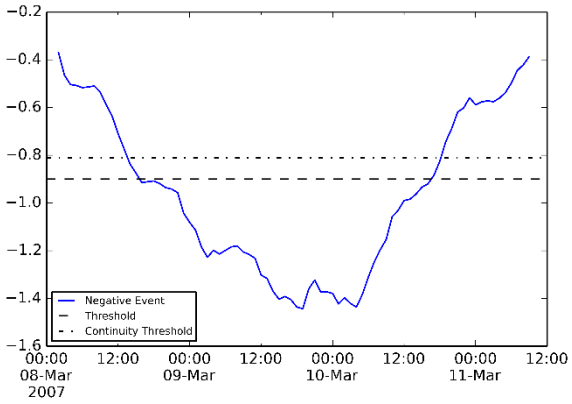

Classification – Type C

2007 Season

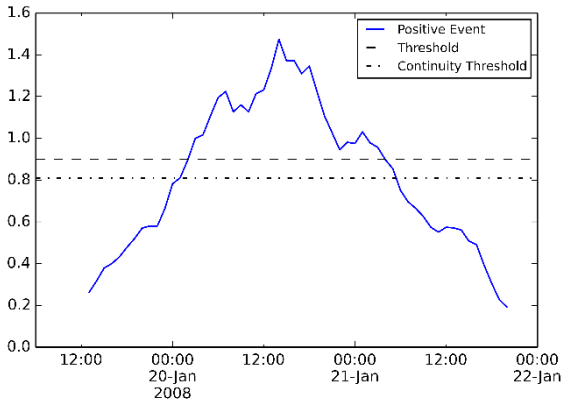

Classification – Type A

2008 Season

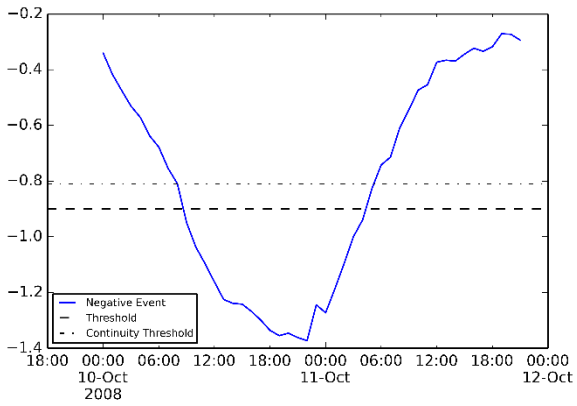

Classification – Type A

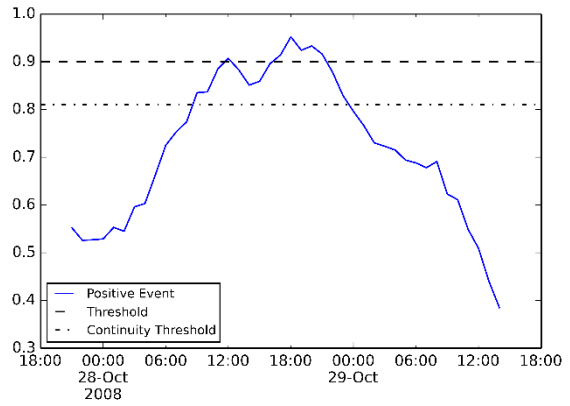

Classification – Type A

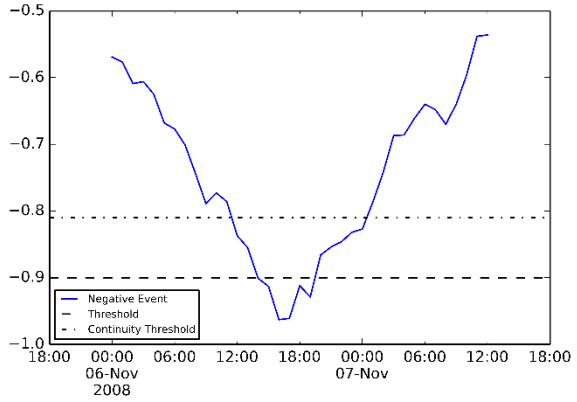

Classification – Type A

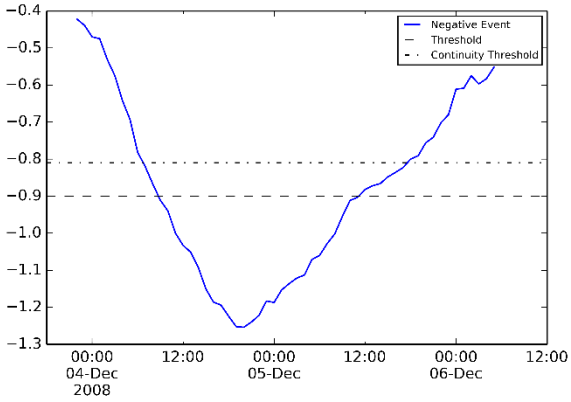

Classification – Type A

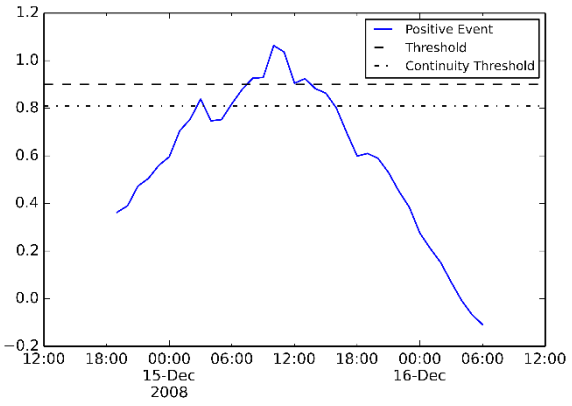

Classification – Type A

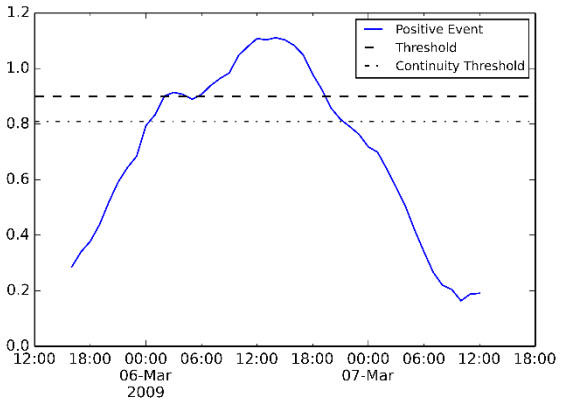

Classification – Type A

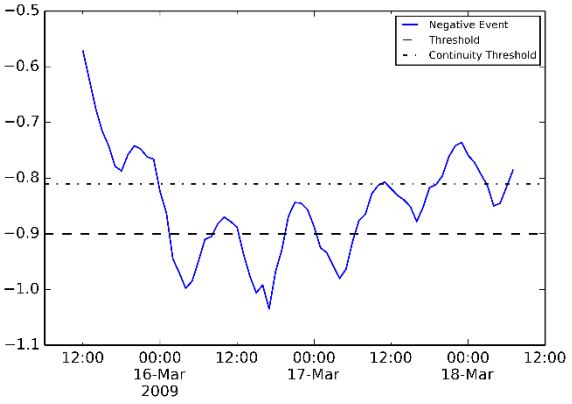

Classification – Type B

2009 Season

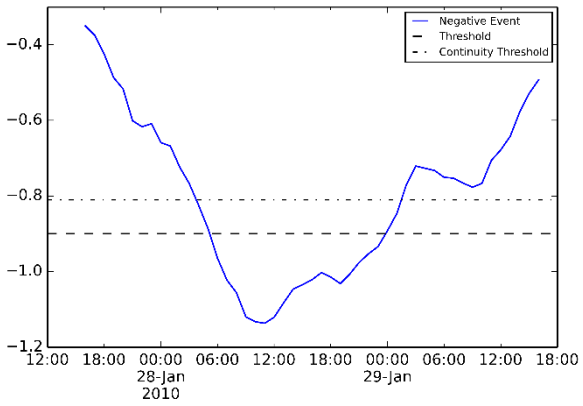

Classification – Type A

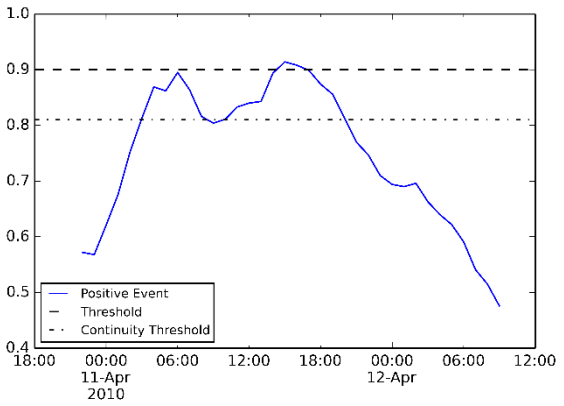

Classification – Type C

2010 Season

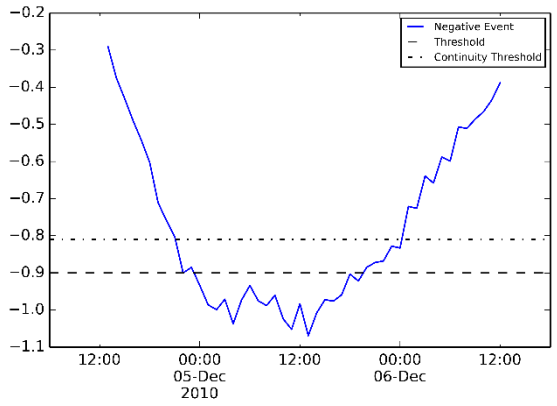

Classification – Type C

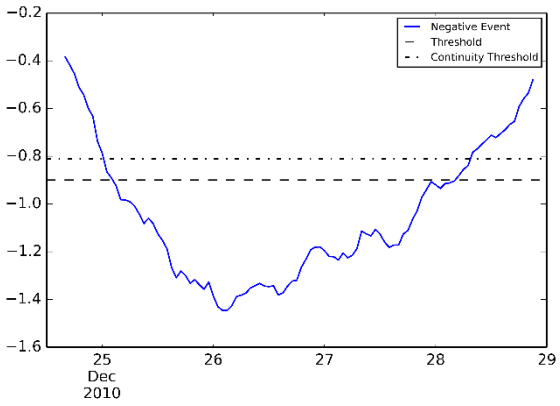

Classification – Type B

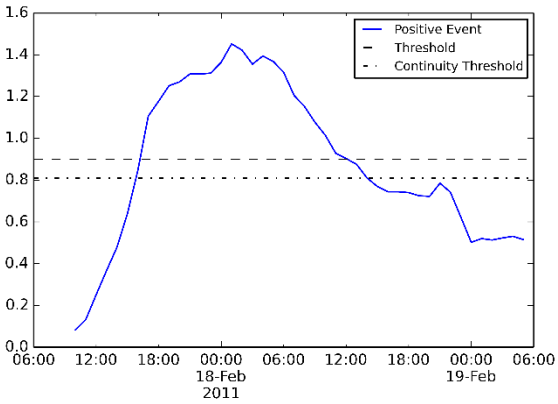

Classification – Type B

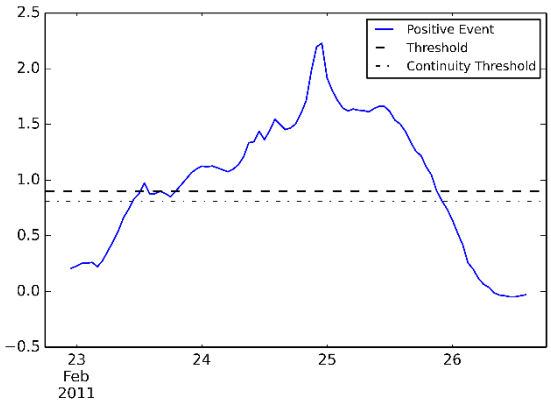

Classification – Type D

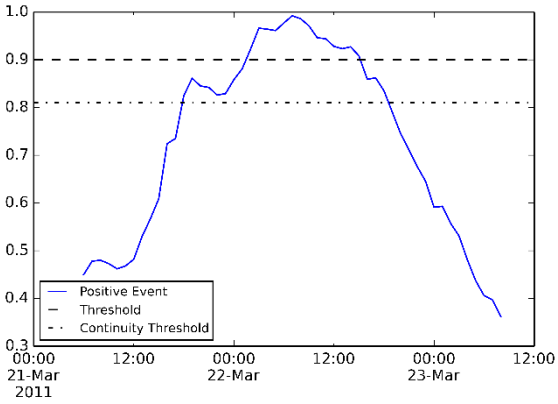

Classification – Type A

2011 Season

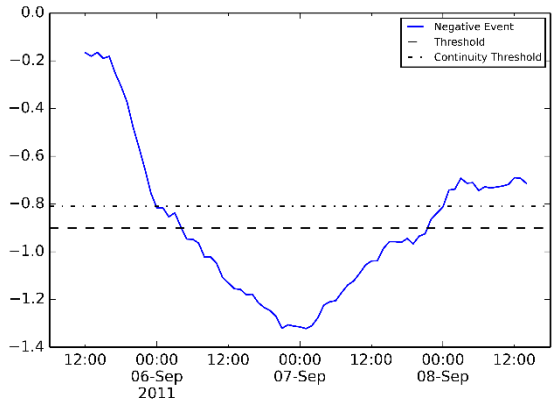

Classification – Type B

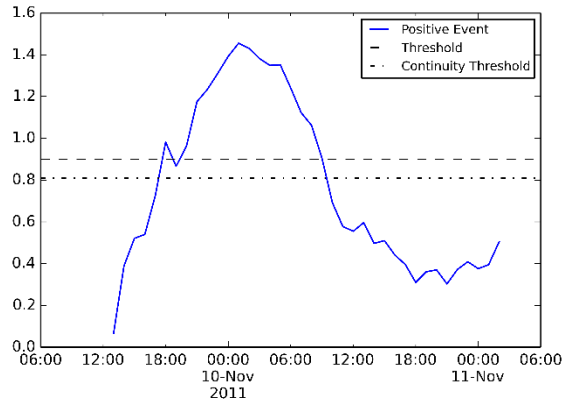

Classification – Type A

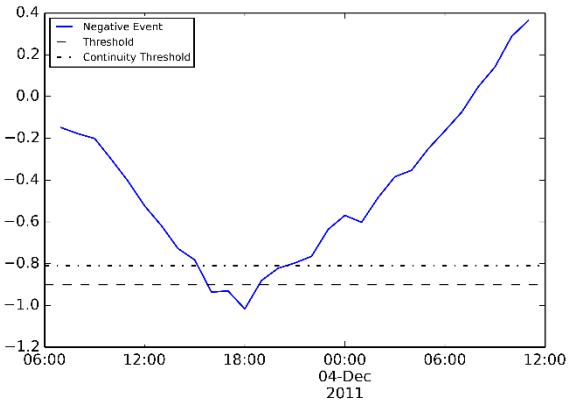

Classification – Type A

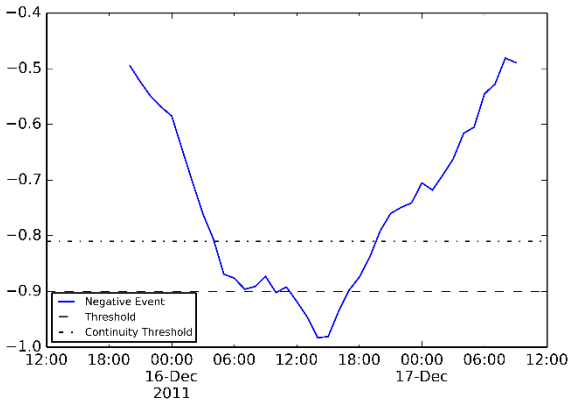

Classification – Type A

2012 Season

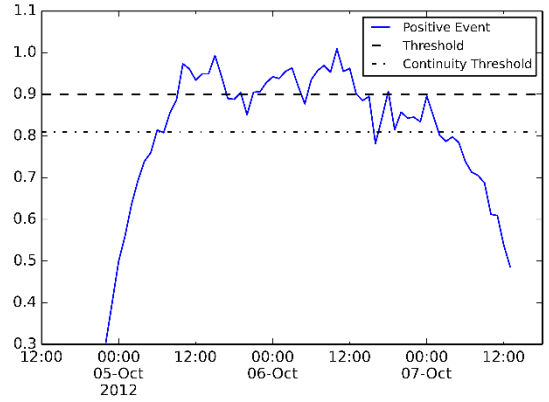

Classification – Type C

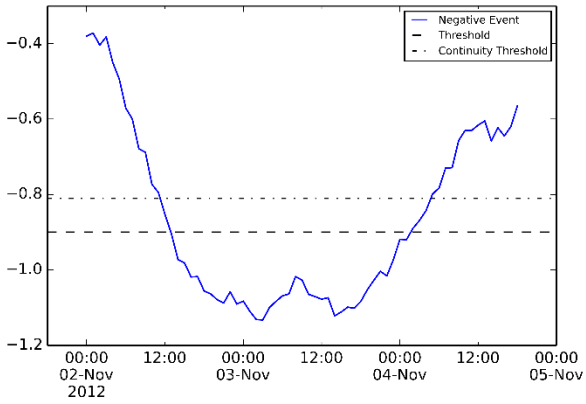

Classification – Type C

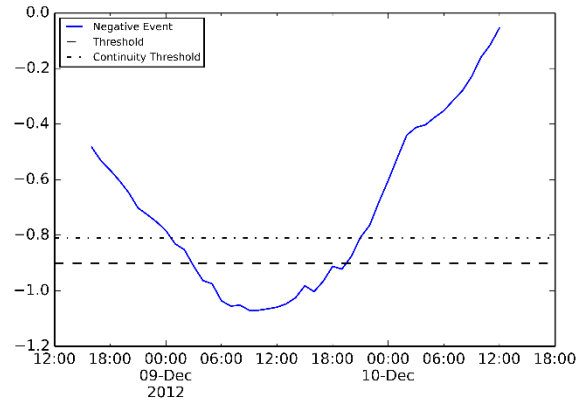

Classification – Type C

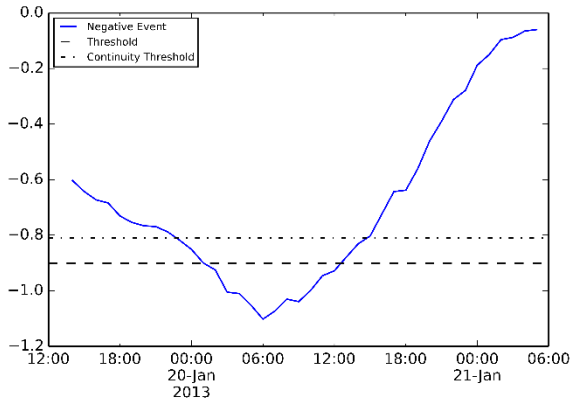

Classification – Type A

2013 Season

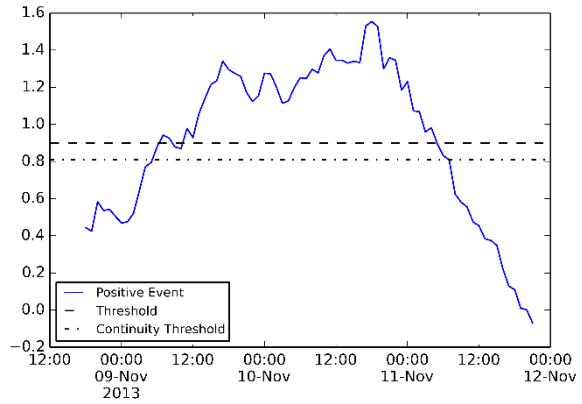

Classification – Type C

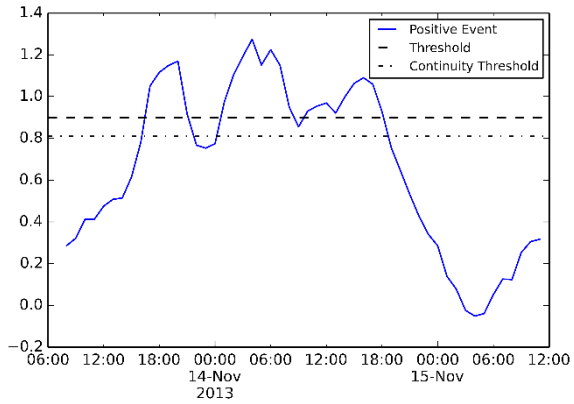

Classification – Type C

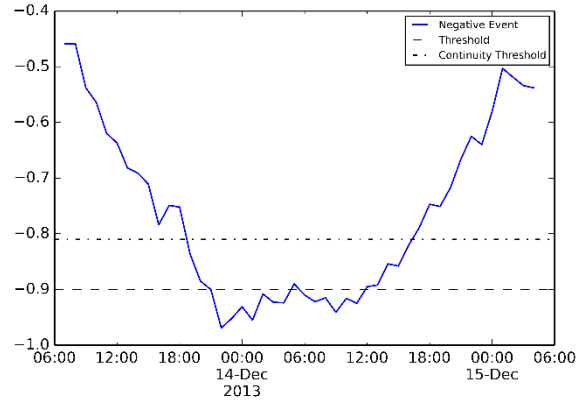

Classification – Type C

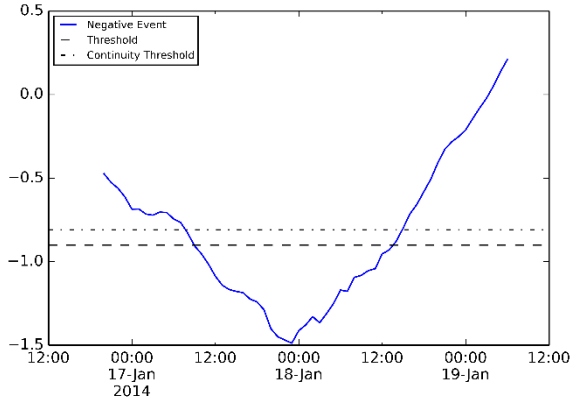

Classification – Type A

Appendix B

Python scripts created for the identification of storm surge events at Red Dog Dock, Alaska, 2004-2014.

```
##Event Algorithm
# trigger threshold ## the residual values must be greater than this to be kept:
THRESHOLD = 0.9
# continuity threshold
CTHRESHOLD = 0.9 * THRESHOLD
# residual values to be added either side of an event
SHOULDER = 12
# max allowable space below threshold to remain a single event
LULL = 6
# shoulder cut off ## consecutive drops BEFORE event threshold is crossed
INCLINE = 9
# shoulder cut off ## consecutive drops AFTER event threshold is crossed
DECLINE = 9
# variable equal to residual
r = dog['datum']
residual = r
# fill T with true/false to keep each value ## tag all values above the threshold
T = []
for x in residual:
        if x < -THRESHOLD or x > THRESHOLD:
                T.append(1)
        else:
                T.append(0)
# fill F with zeroes where the value is under the threshold and residual values for T == 1
F = []
for x in range(len(residual)):
        F.append(residual[x]*T[x])
# add in the residual values surrounding each event
i = 0
while i < len(T):
        if T[i] == 1:
                j = 0
                while abs(residual[i-j]) >= CTHRESHOLD:
                        F[i-j] = residual[i-j]
                        j += 1
                x = 0
                more = 0
                while x < SHOULDER and more < INCLINE:
                        F[i-j] = residual[i-j]
                        if residual[i-j]*residual[i-j-1] <= 0:
                                break
                        if abs(residual[i-j]) > abs(residual[i-j-1]):
                                more +=1
                        else:
                                more = 0
                        x +=1
                        j +=1
                n = 1
```

```
        while (n < LULL or abs(residual[i+n]) >= CTHRESHOLD) and i+n < len(T):
                F[i+n] = residual[i+n]
                if T[i+n] == 0:
                        n += 1
                        continue
                else:
                        i += n
                        n = 0
                n += 1
        i += n
        x = 0
        less = 0
        while x < SHOULDER and less < DECLINE:
                F[i] = residual[i]
                if abs(residual[i]) <= abs(residual[i+1]):
                        less += 1
                else:
                        less = 0
                x += 1
                i += 1
i += 1
```